Remote Sensing of Tropical Cyclones by SAR and Constellation

Past, Present and Future

Biao Zhang

Contributors: Yijun He, Shengren Fan, Kangyu Zhang, NUIST
William Perrie, BIO
Alexis Mouche, IFREMER
Vladimir Kudryavtsev, RSHU

High wind speeds are underestimated in the eyewall regions of tropical cyclones, due to the saturation of VV-polarized radar backscattering when wind speeds approach to hurricane force.

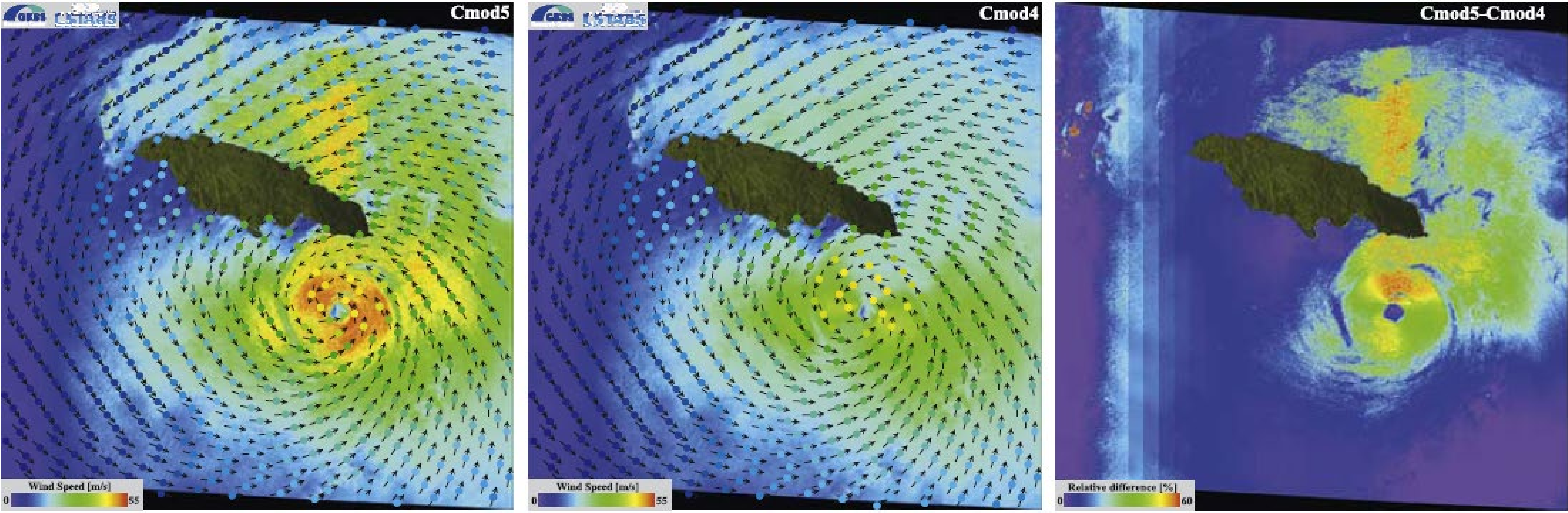

Horstman et al. 2005, GRL

- Cross-polarized radar backscattering is not sensitive to incidence angle and wind direction, but increases with increasing wind speed, particularly for high winds.

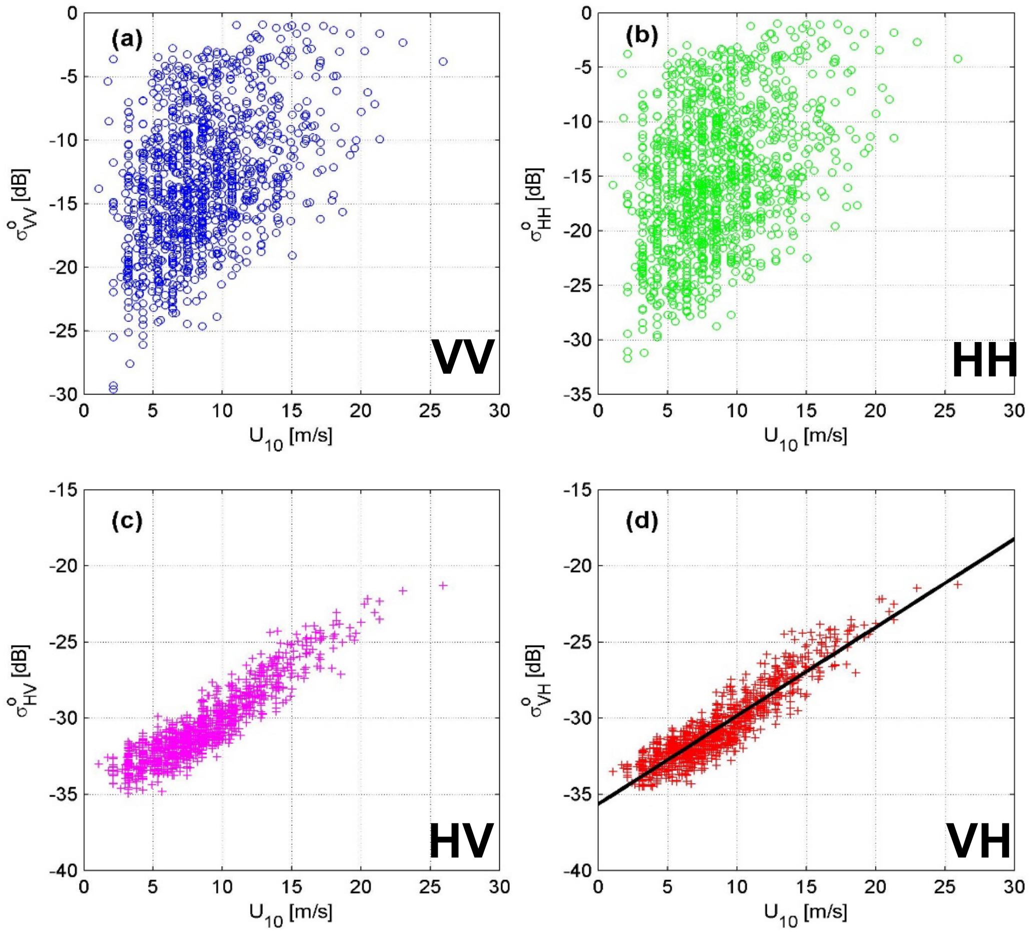

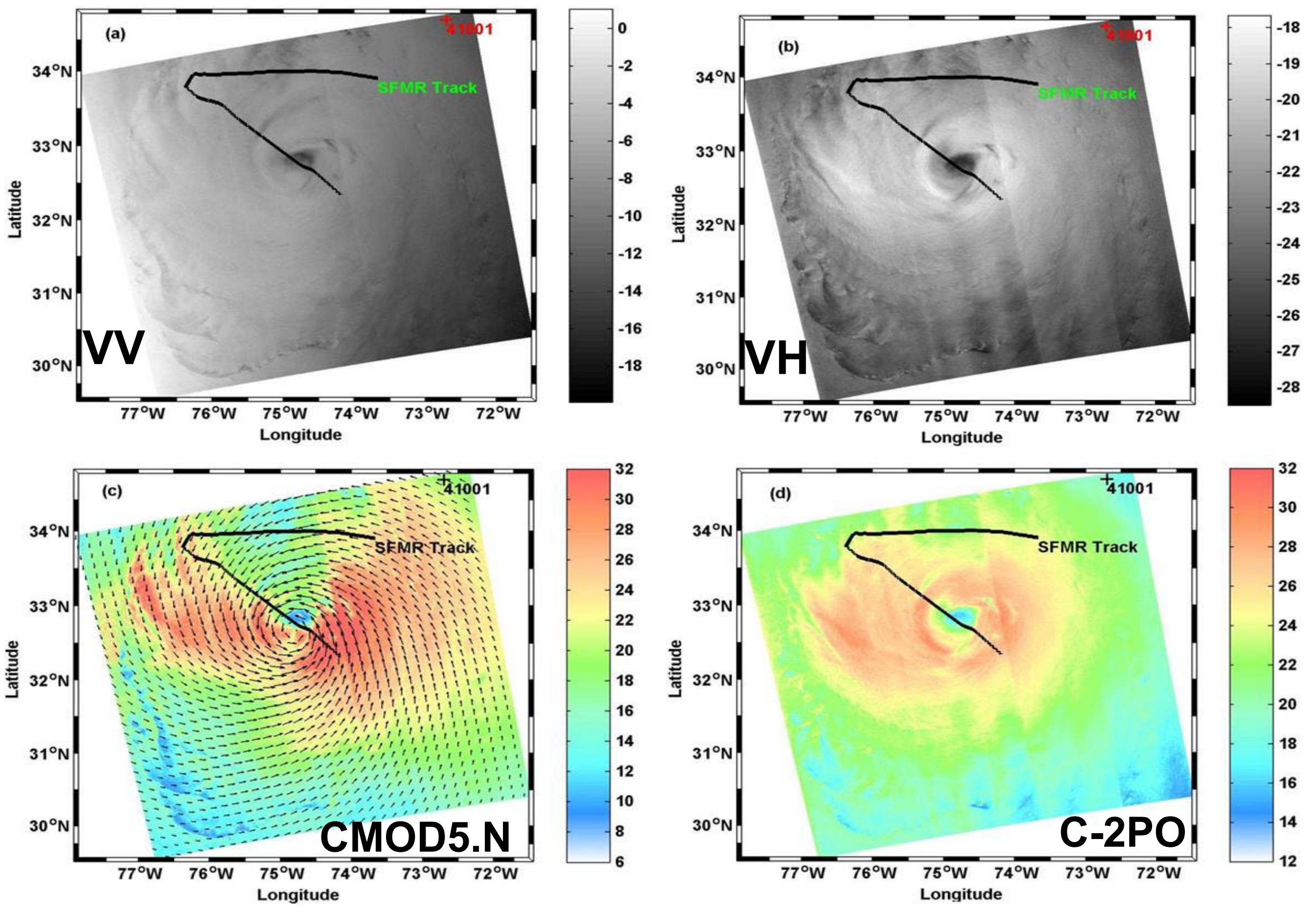

Zhang & Perrie 2012, BAMS

- TC surface wind vectors can be derived using co- and cross-polarized SAR images, but with wind direction ambiguity.
- The wind direction ambiguities are removed using a parametric two-dimensional sea surface inflow angle model.

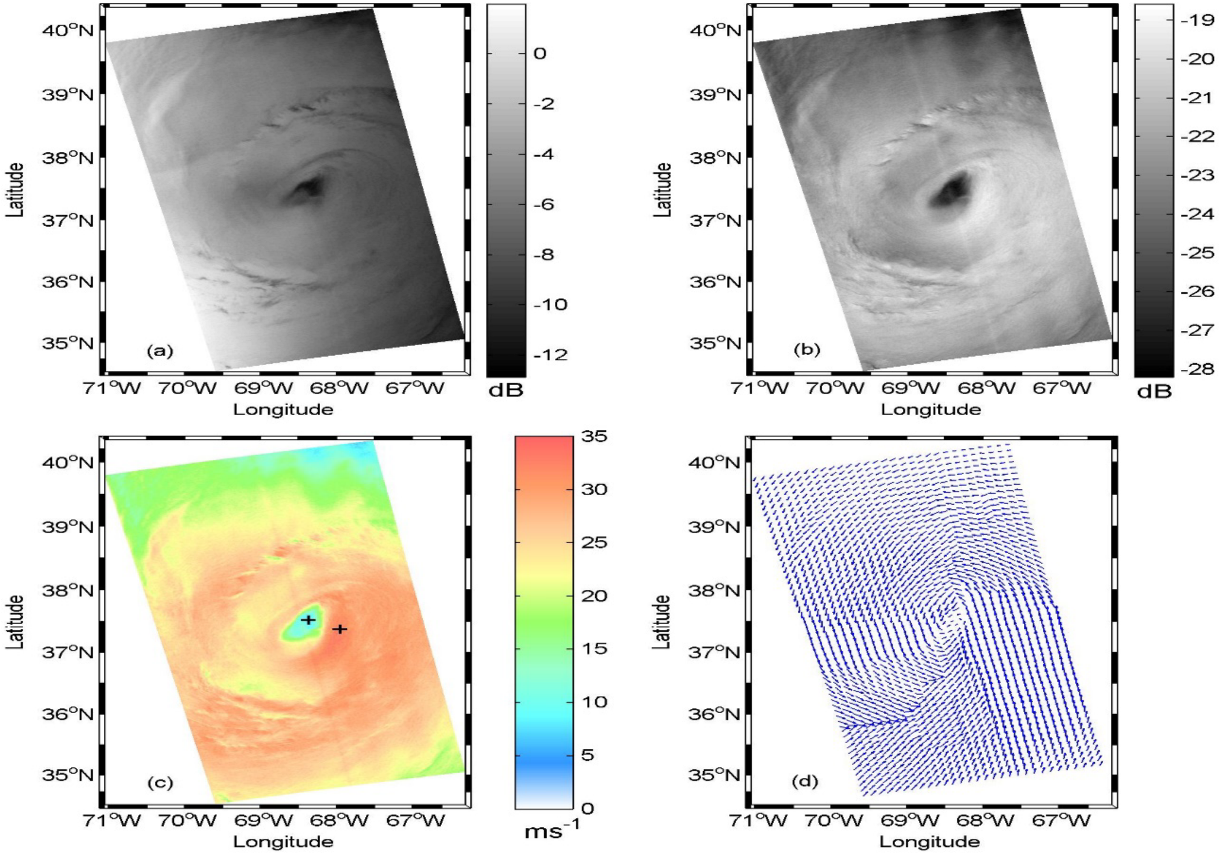

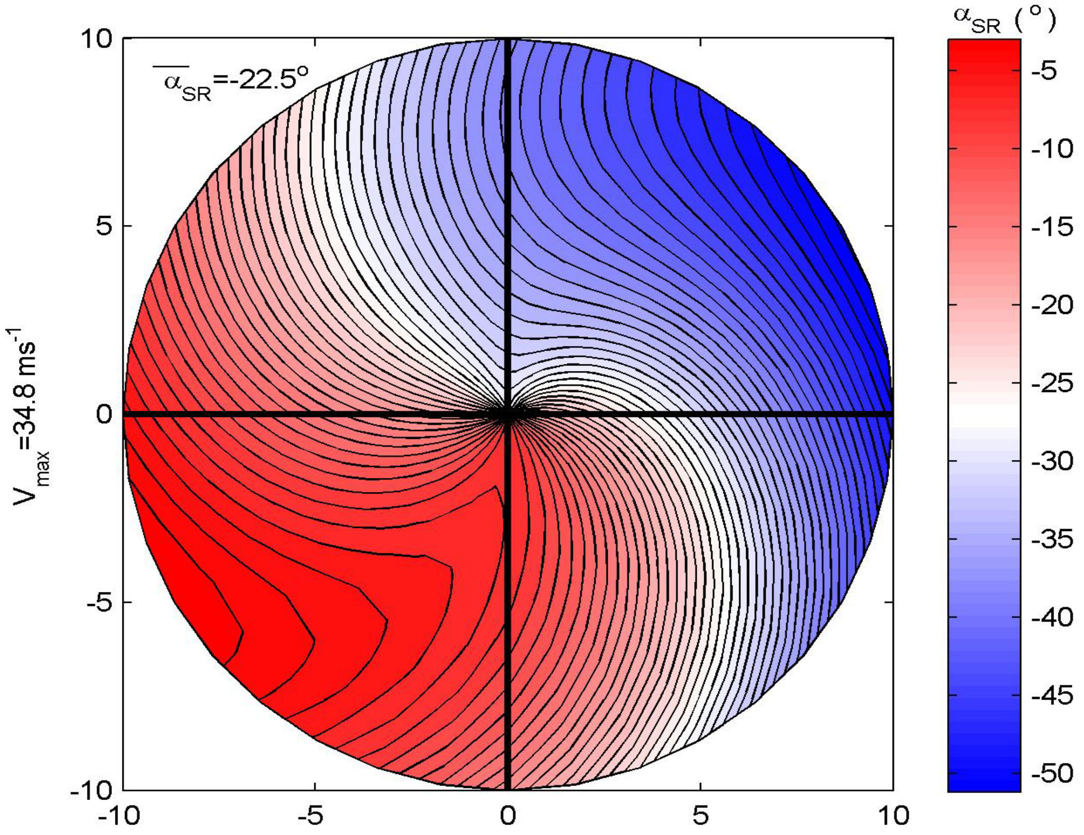

Zhang et al. 2014, JTECH

- Cross-polarized GMF was updated by both considering both the dependence of incidence angle and wind speed.
- The inner and outer core regions of TCs are both accurately retrieved when VV- and VH-polarized SAR images are used.

$$J(u,v) = \left[\frac{\sigma_{VV}^{o} - \sigma_{VV}^{s}}{\Delta\sigma_{VV}}\right]^2 + \left[\frac{\sigma_{VH}^{o} - \sigma_{VH}^{s}}{\Delta\sigma_{VH}}\right]^2 + \left[\frac{u_{ECMWF} - u}{\Delta u}\right]^2 + \left[\frac{v_{ECMWF} - v}{\Delta v}\right]^2$$

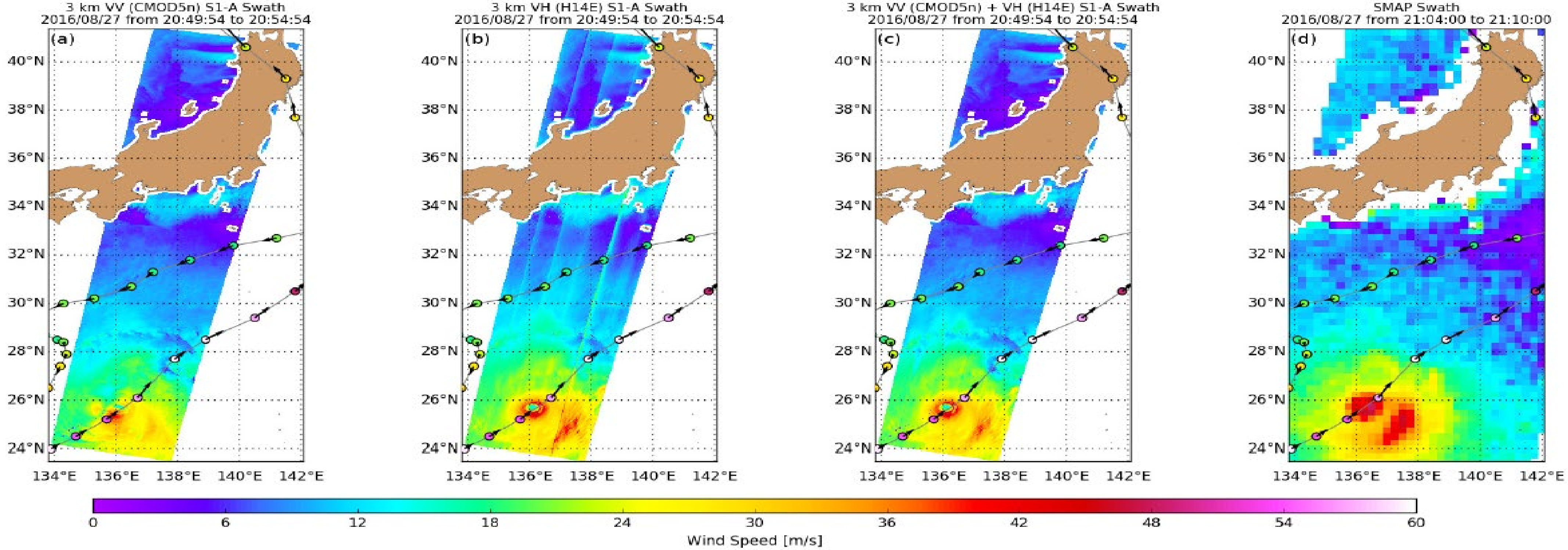

Mouche & Zhang et al. 2017, IEEE TGRS

- The wind speeds from dual-polarized SAR images are compared with collocated SFMR measurements, showing a bias of 2 m/s and a RMSE of 5 m/s.

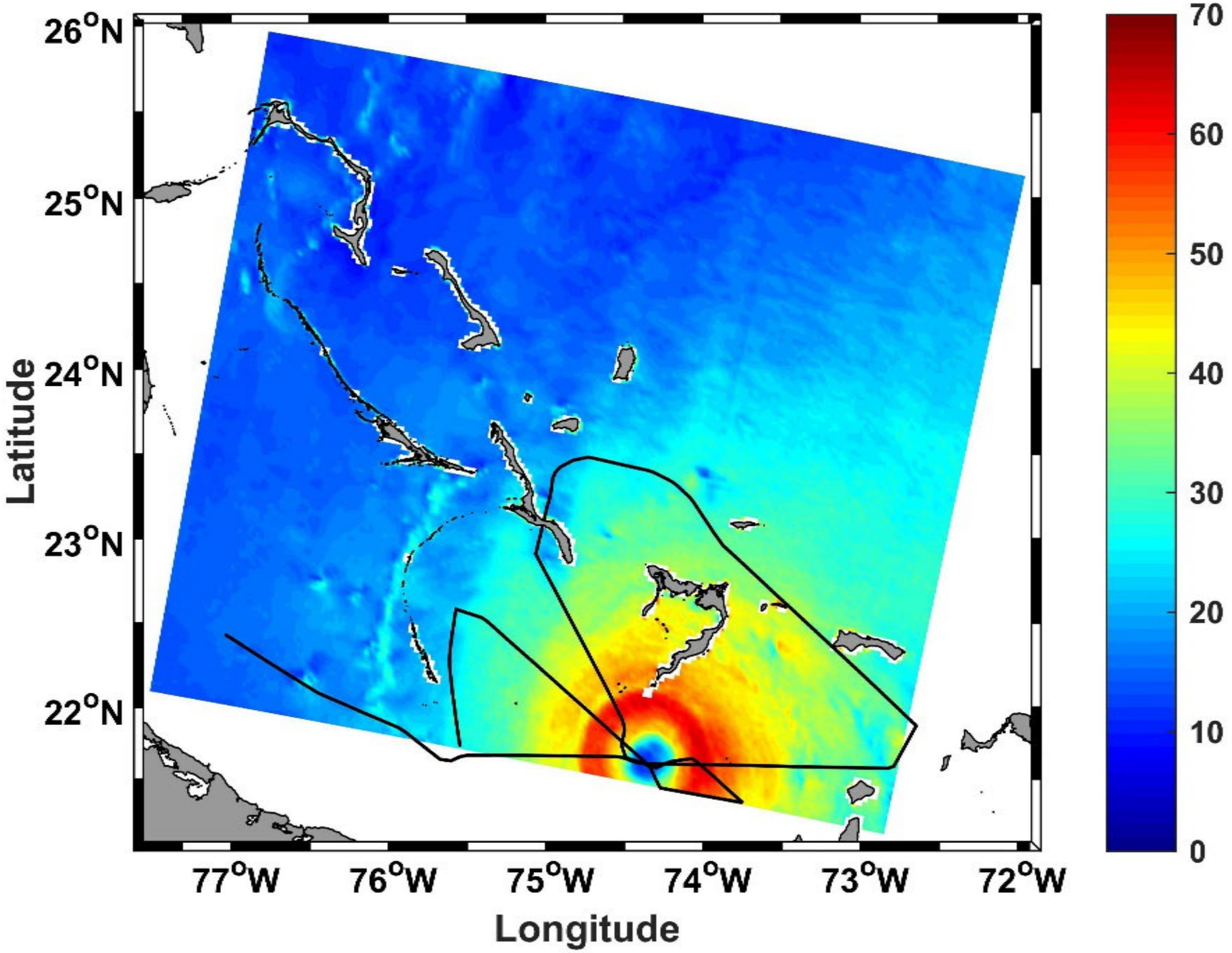

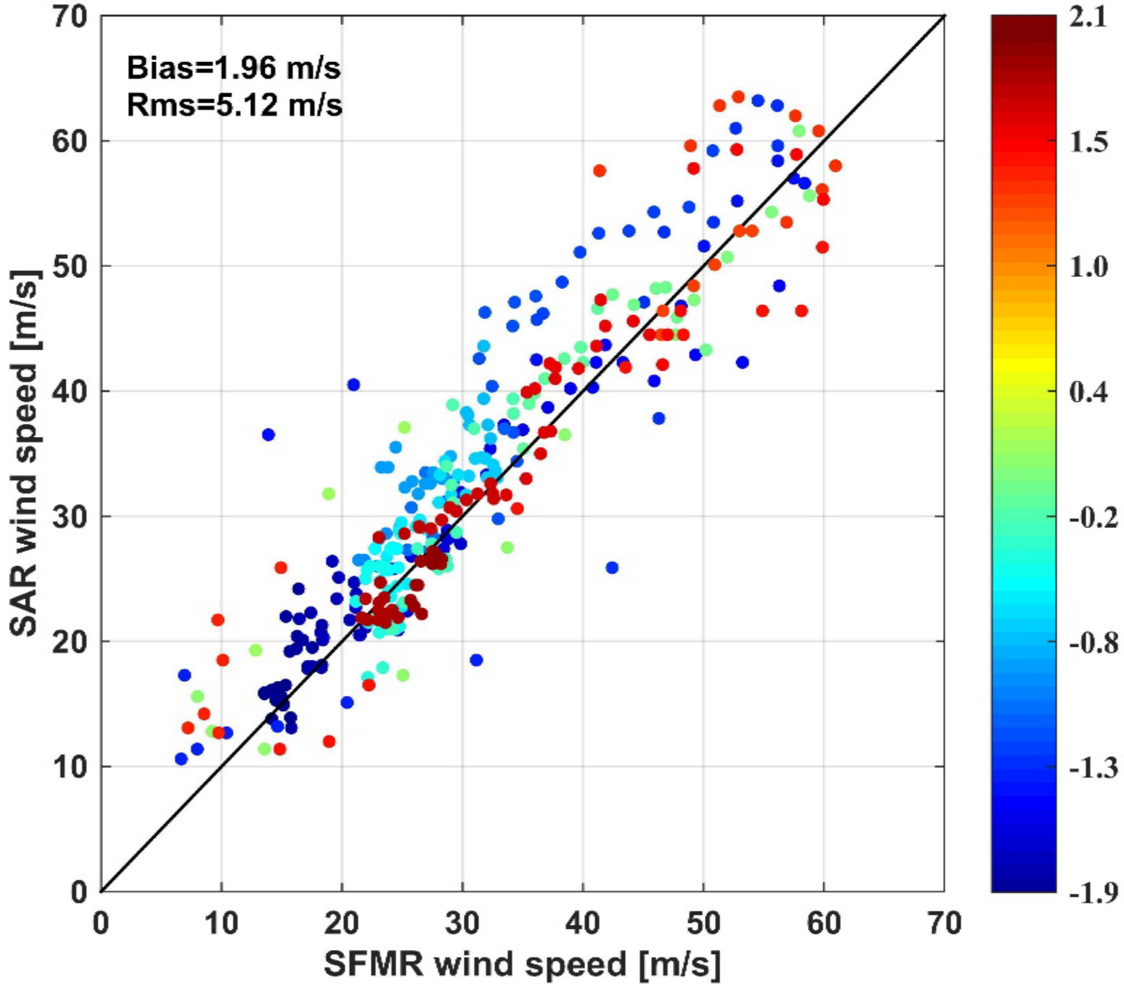

- The thermal noise exisinting in Sentinel-1 SAR images acquired in TOPSAR mode should be eliminated, prior to wind speed retrieval.

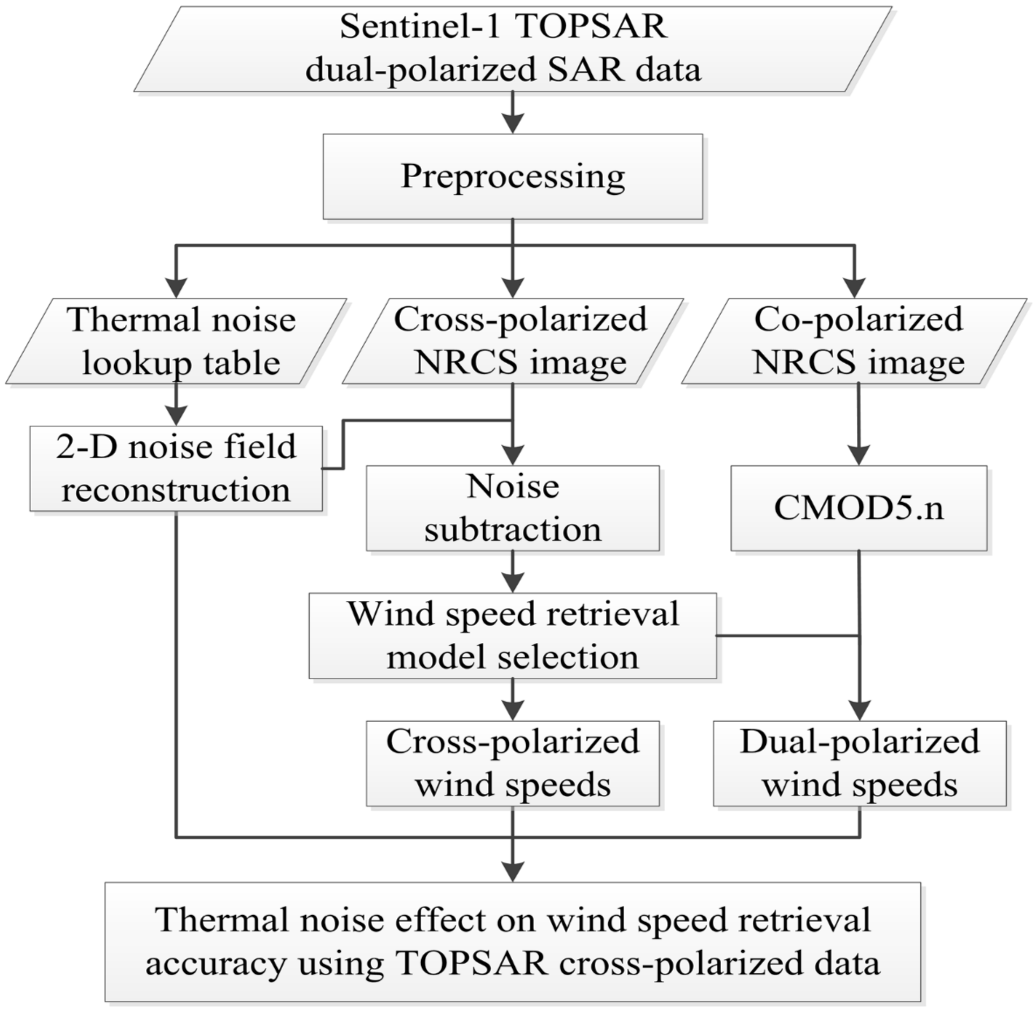

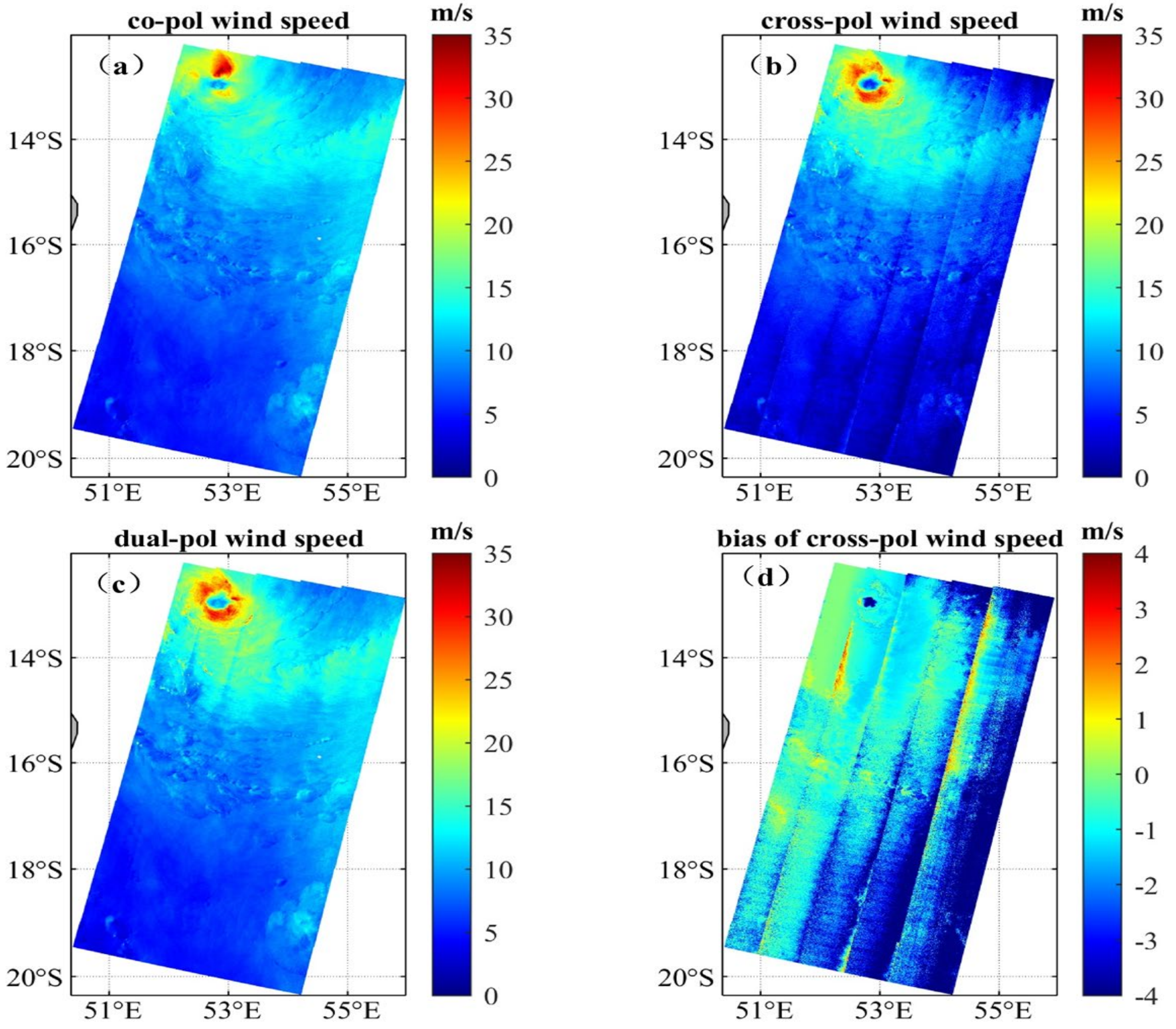

Zhang et al. 2023, IEEE TGRS

- VH-polarized SAR imagery captures the structural features of storms well and shows prominent image gradients along the radial directions of the storm.
- The signal-to-noise ratios of VH-polarized images are small in low wind speed areas, but they are large in the same regions of VV-polarized images.

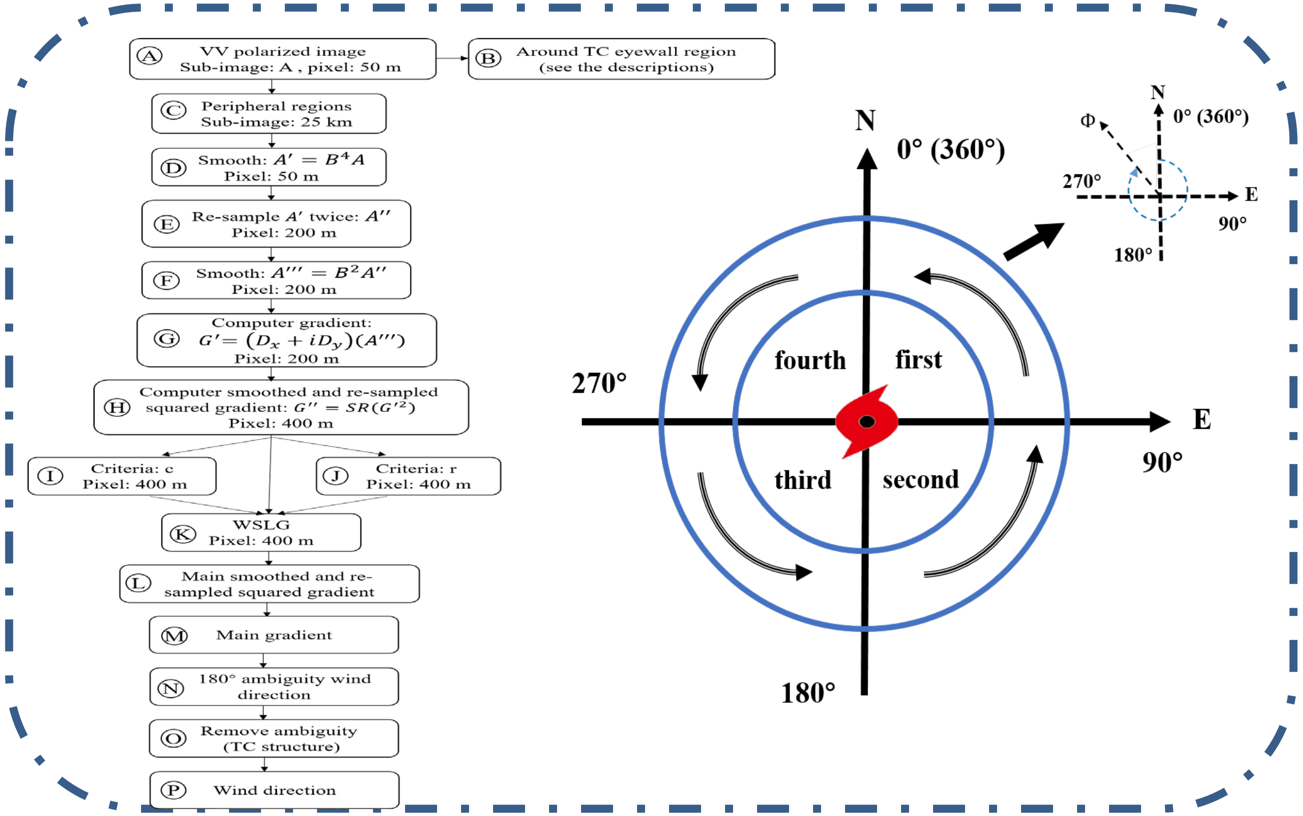

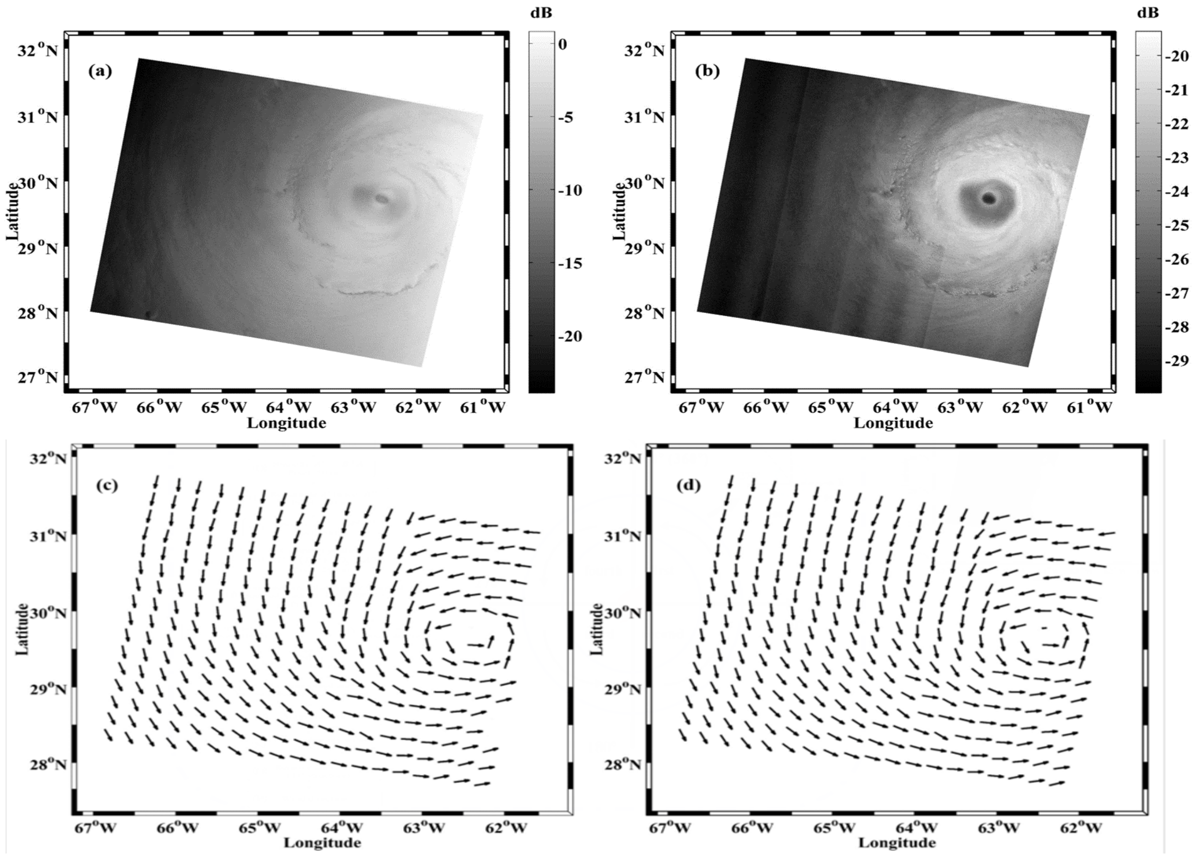

Fan & Zhang et al. 2020, IEEE TGRS

- dual-polarization SAR is more suitable for the estimation of TC wind directions than VV- or VH-polarization SAR.

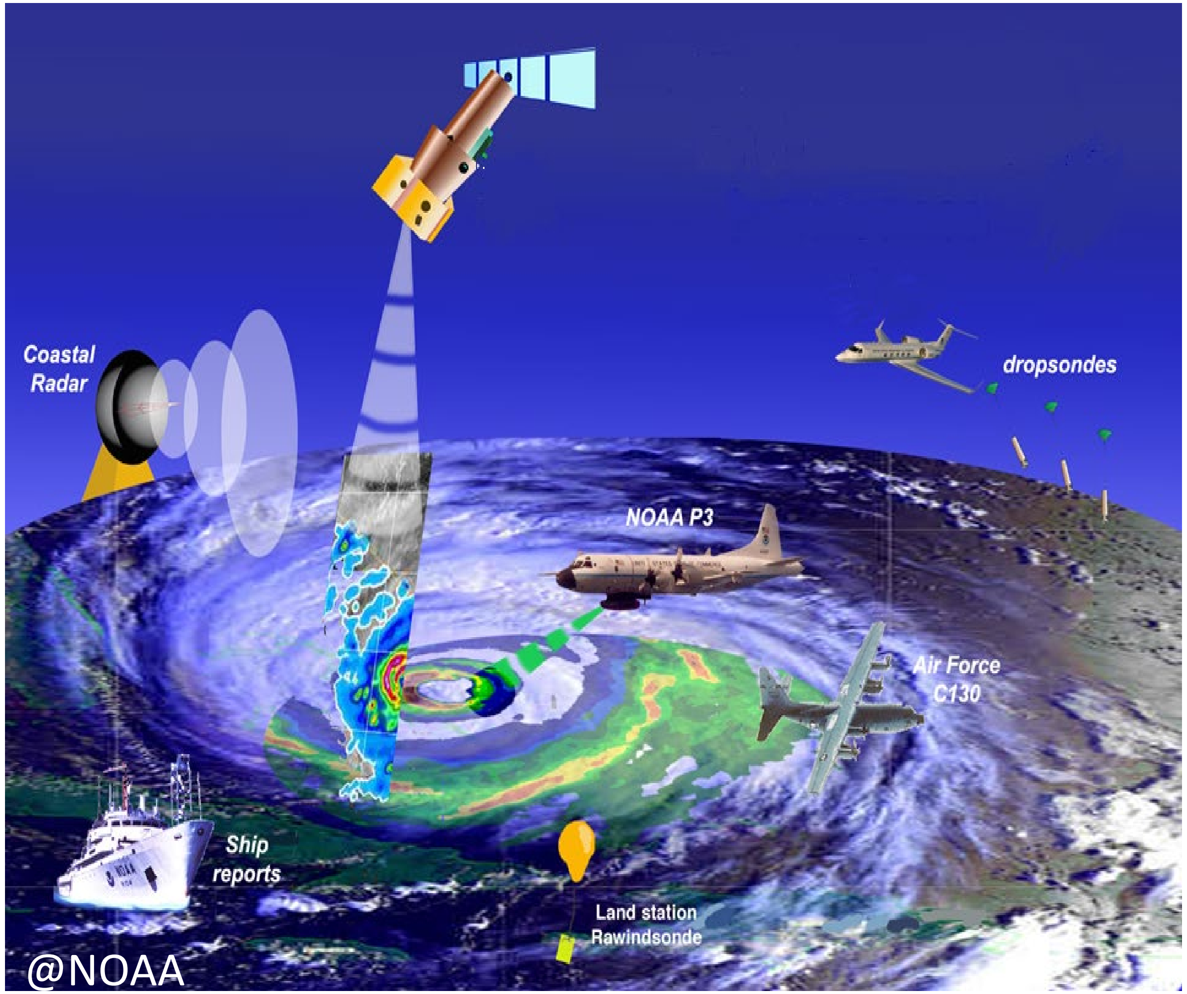

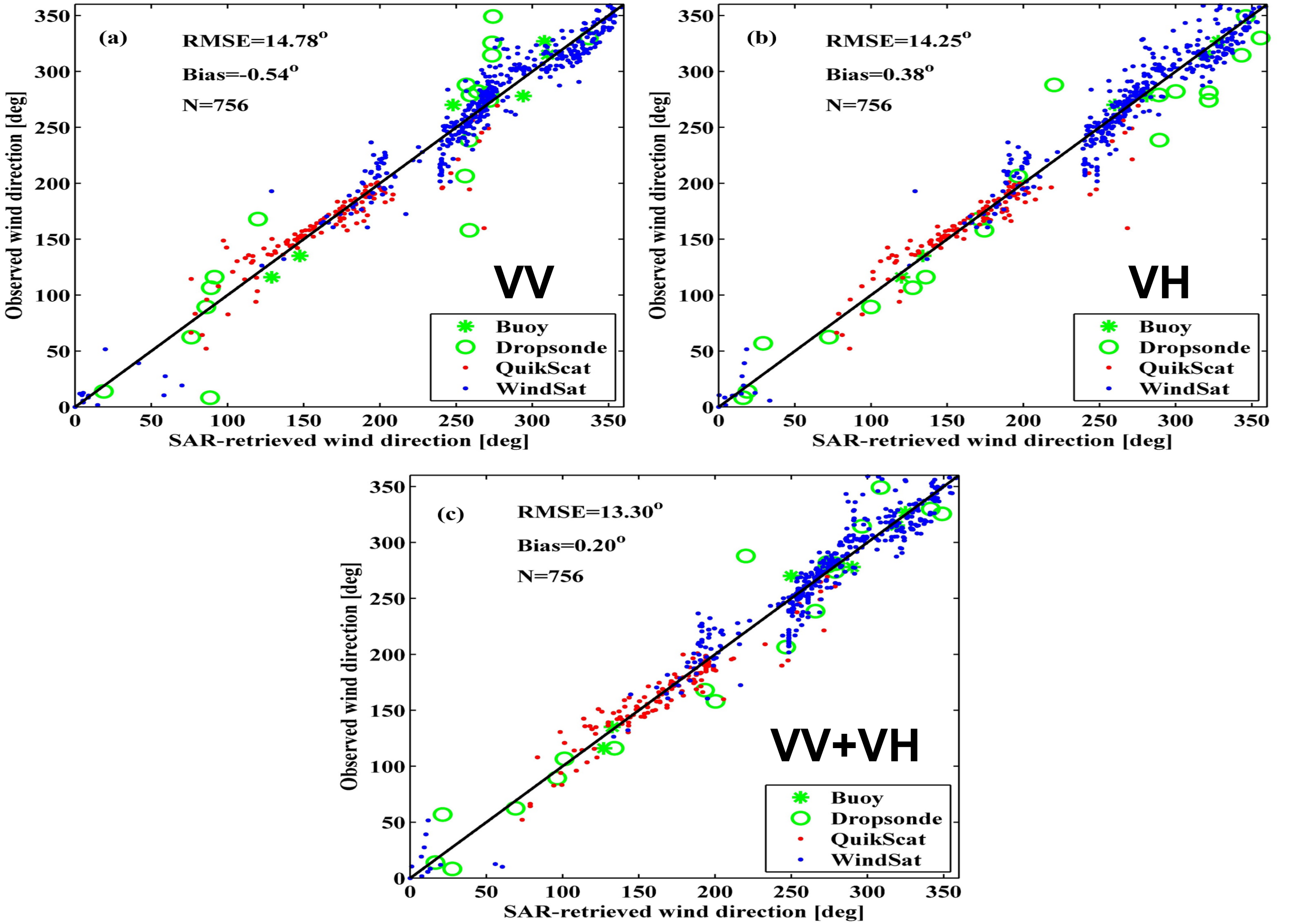

- Cross-polarized radar backscatterings simulated by the composite surface Bragg (CB) theory model are underestimated. This is because the second-order contributions of the Bragg wave were ignored.

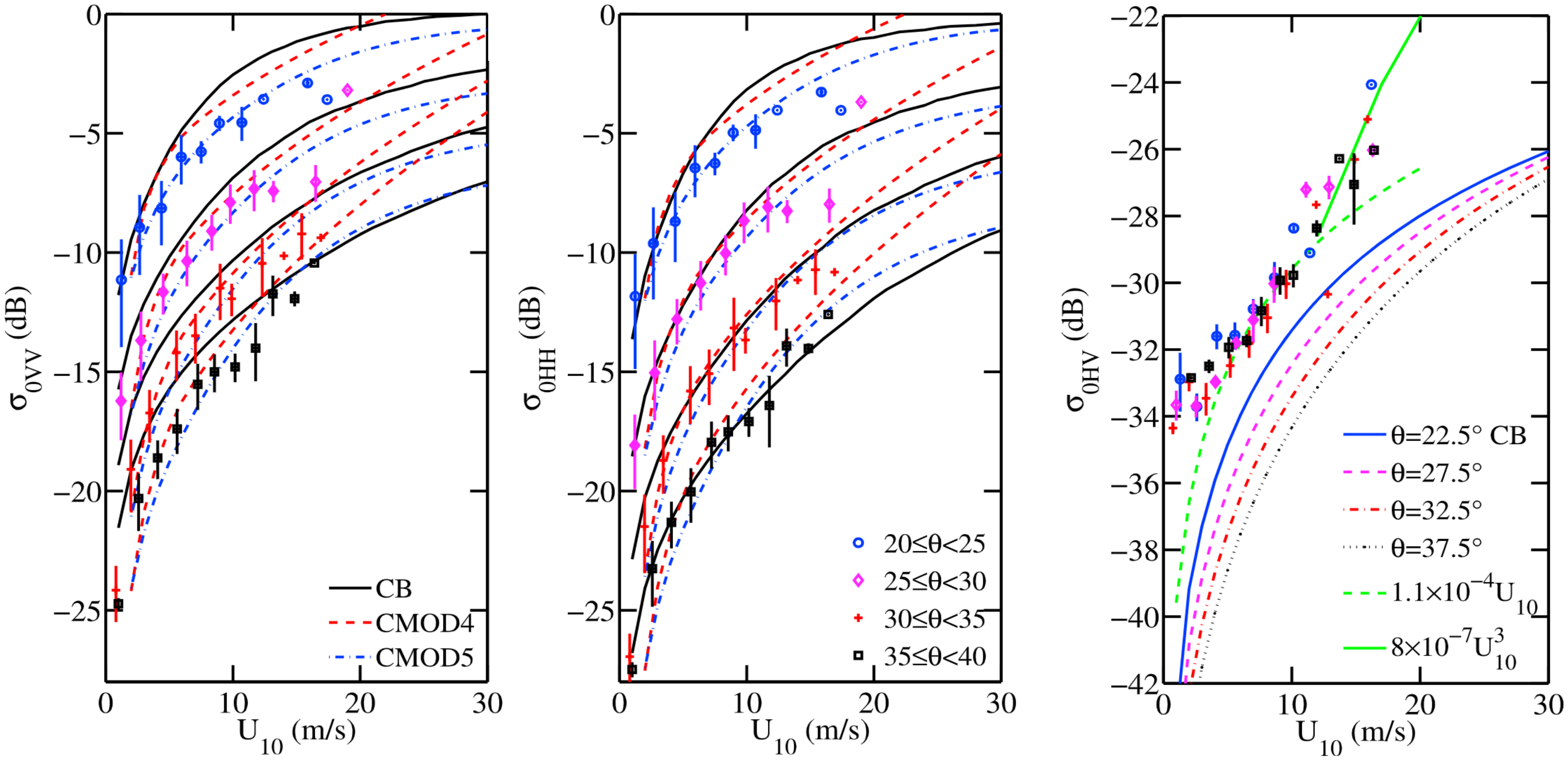

Hwang & Zhang et al. 2010, JGR

- For VV polarized measurements, the contribution of breaking waves decreased from 60% to 20% with increasing incidence angle, whereas for HH polarization and cross-polarization measurements, it can amount to about 60%–70% for all incidence angles.

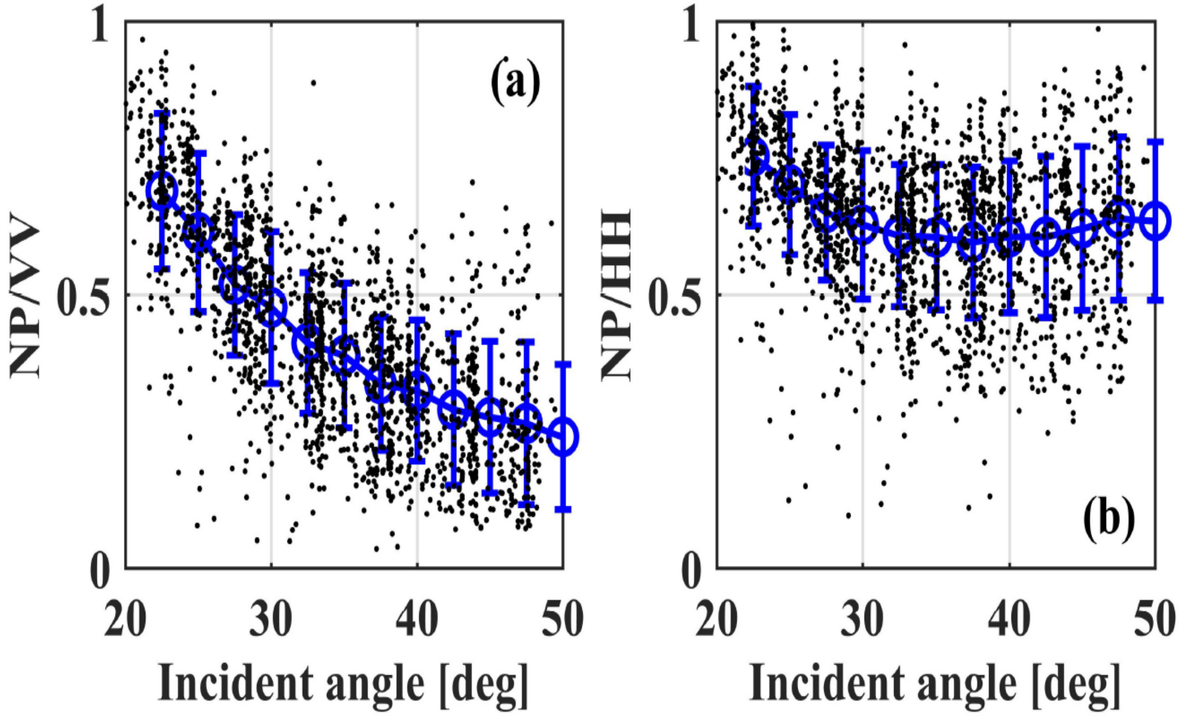

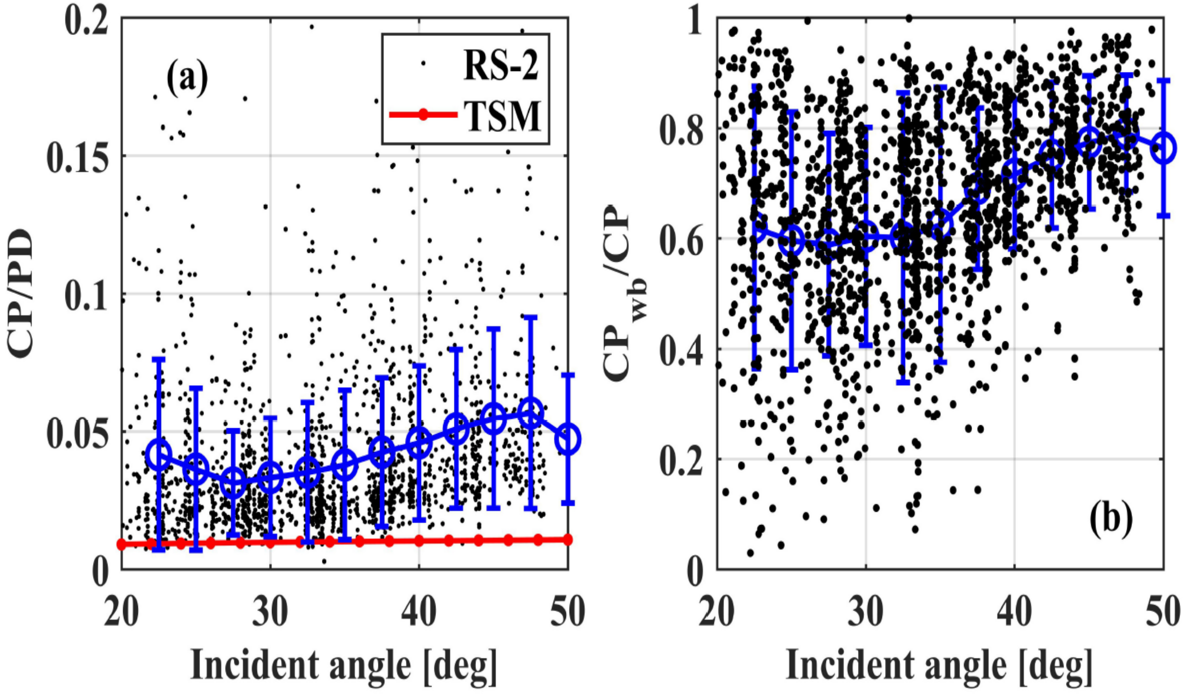

Kudryavtsev and Zhang et al. 2019, TGRS

- Simulations of quad-polarization radar backscatter are significantly improved when the effects of breaking waves are incorporated, especially for HH and VH polarizations.

microwave scattering theoretical model for regular waves:

$$S_{\alpha\alpha_0}\left(\vec{k},\overrightarrow{k_0}\right) = \frac{(q_k q_0)^{1/2}}{2\pi^2(q_k+q_0)}\int\left[B\left(\vec{k},\overrightarrow{k_0}\right) - i\int M\left(\vec{k},\overrightarrow{k_0};\vec{\xi}\right)\tilde{h}\left(\vec{\xi}\right)exp\left(i\vec{\xi}\vec{r}\right)d\vec{\xi}\right] \cdot \exp\left[i\left(\overrightarrow{k_0}-\vec{k}\right)\vec{r} + i(q_k+q_0)h(\vec{r})\right]d\vec{r}$$

$$M\left(\vec{k},\overrightarrow{k_0};\vec{\xi}\right) = \frac{1}{4}\left[B_2\left(\vec{k},\overrightarrow{k_0},\vec{k}-\vec{\xi}\right) + B_2\left(\vec{k},\overrightarrow{k_0},\overrightarrow{k_0}+\vec{\xi}\right) + 2(q_k+q_0)B\left(\vec{k},\overrightarrow{k_0}\right)\right]$$

microwave scattering empirical model for breaking waves:

$$\sigma_{wb}^{np}(\theta,U_{10},\varphi) = f_{np}(\theta)U_{10}^{n_{np}}exp\left[A_{0np} + A_{1np}\cos\varphi + A_{2np}\cos 2\varphi\right]$$

$$\sigma_{wb}^{cp}(\theta,U_{10},\varphi) = f_{cp}(\theta)U_{10}^{n_{cp}}exp\left[A_{0cp} + A_{1cp}\cos\varphi + A_{2cp}\cos 2\varphi\right]$$

Zhang et al. 2020, JGR: Oceans

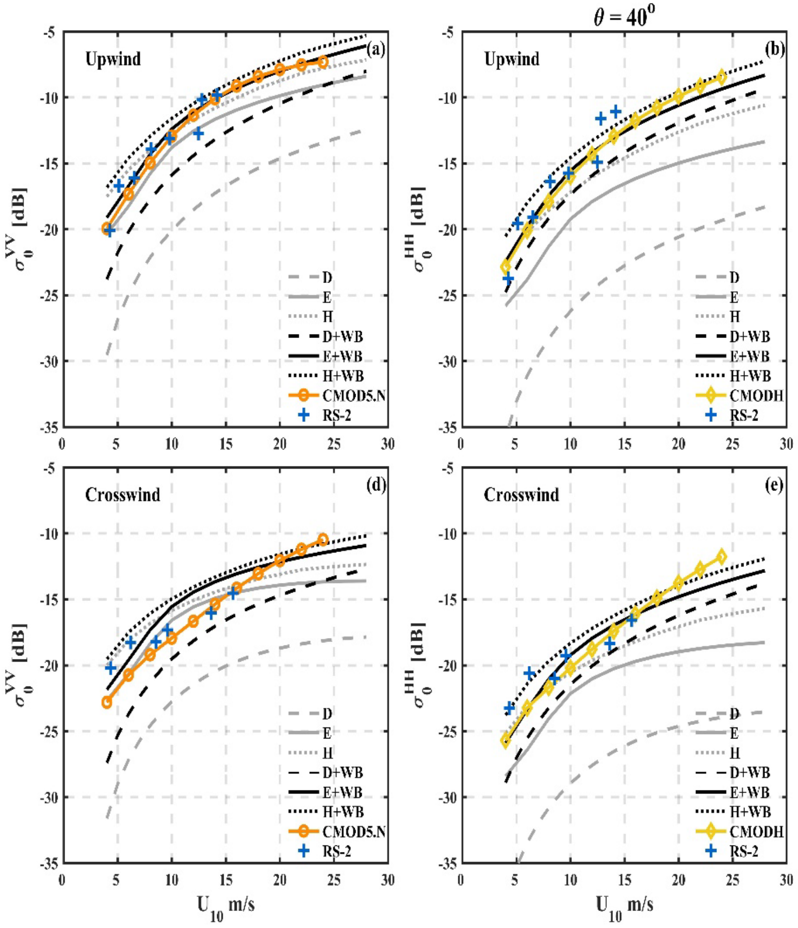

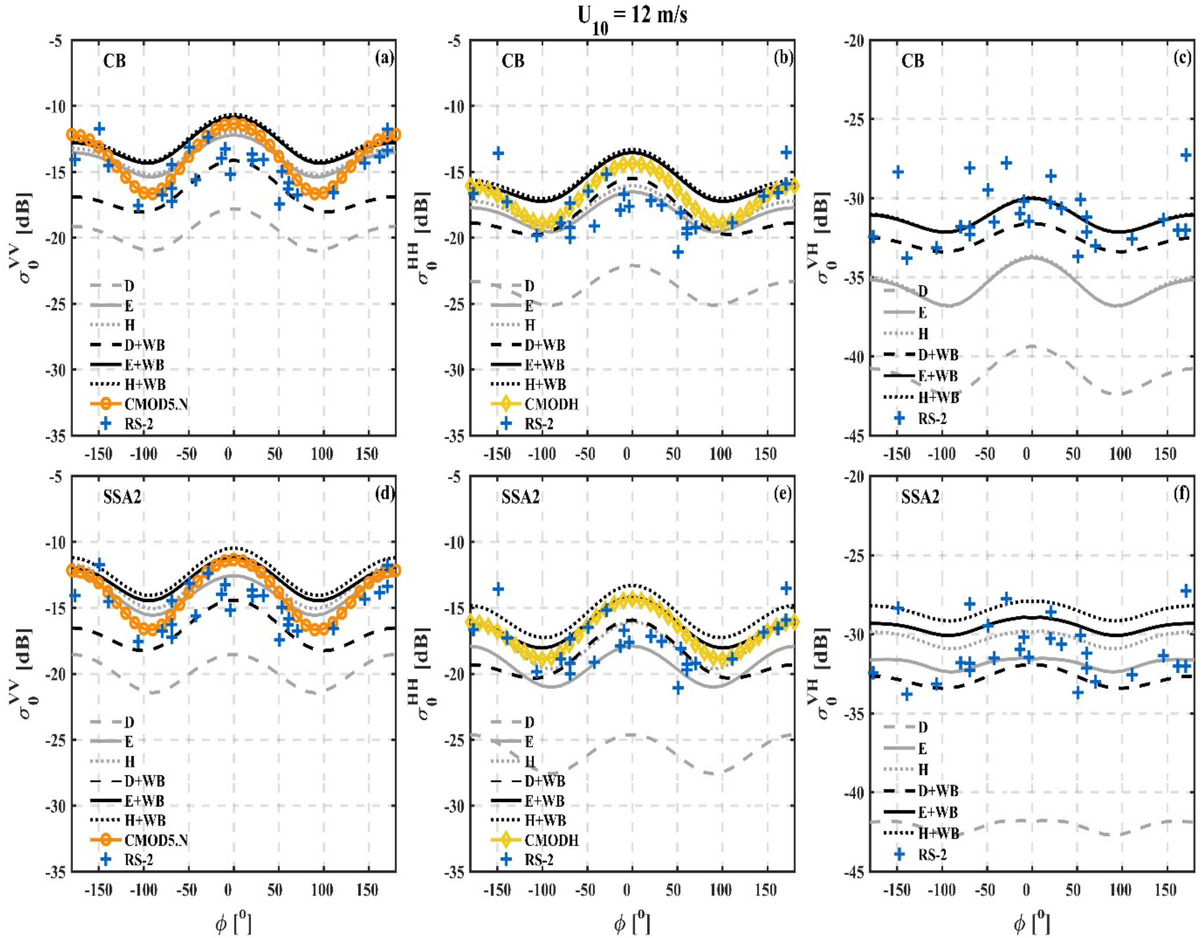

Zhang et al. 2020, JGR: Oceans

- For the first time, quasi-synchronous wide-swath quad-polarization (HH+HV+VH+VV) observations over a hurricane are achieved trhough a virtual constellation.

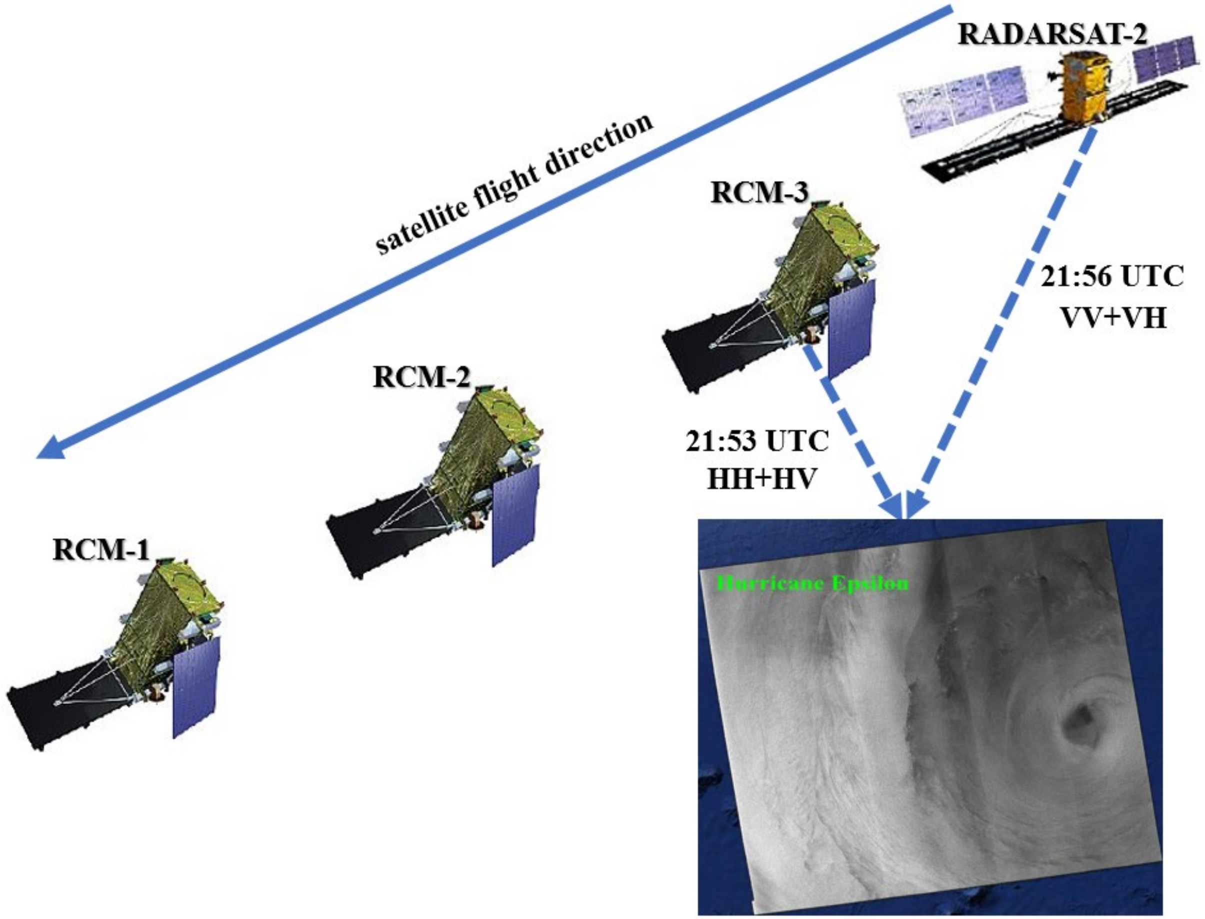

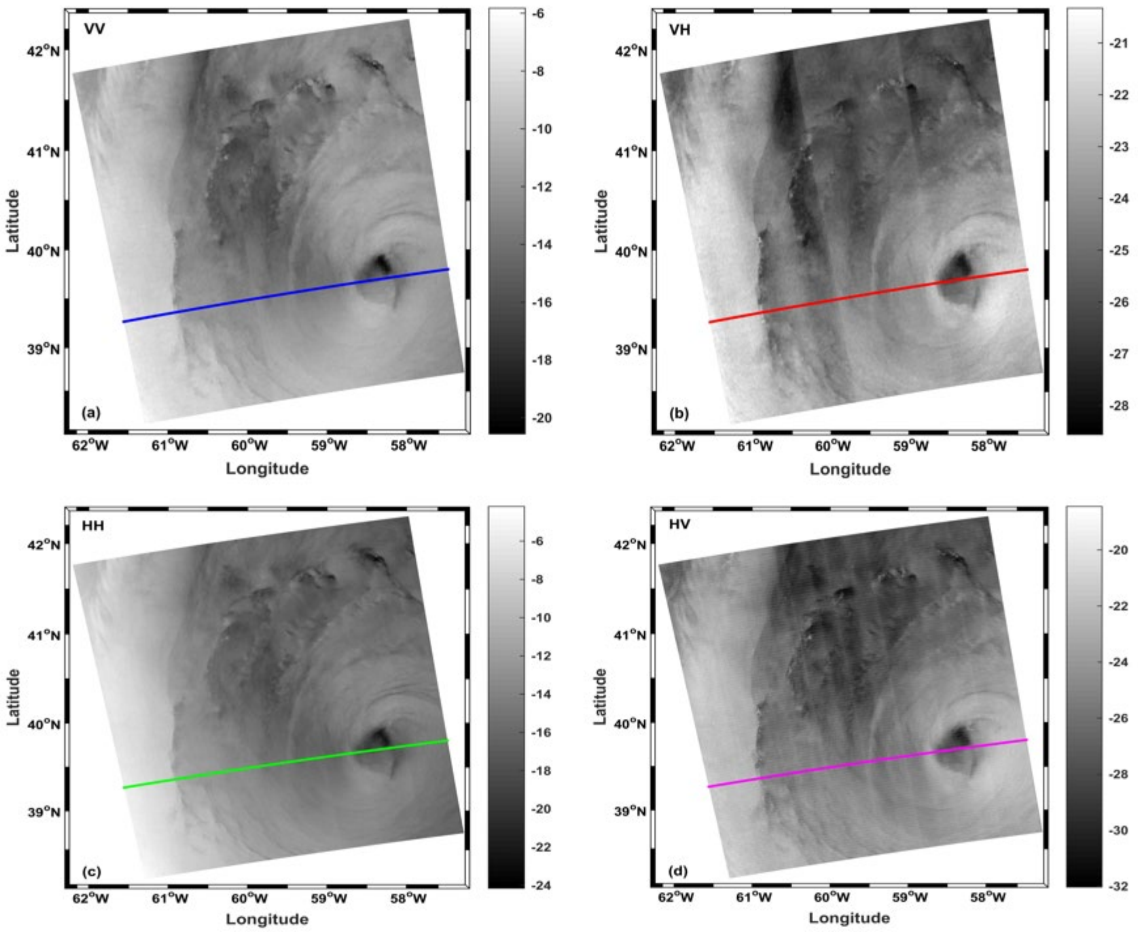

Zhang et al. 2022, IEEE TGRS

- NRCS values at HV- and VH-polarizations are more sensitive to wind speeds and less sensitive to incidence angles or wind directions than those at HH and VV for hurricane force winds.

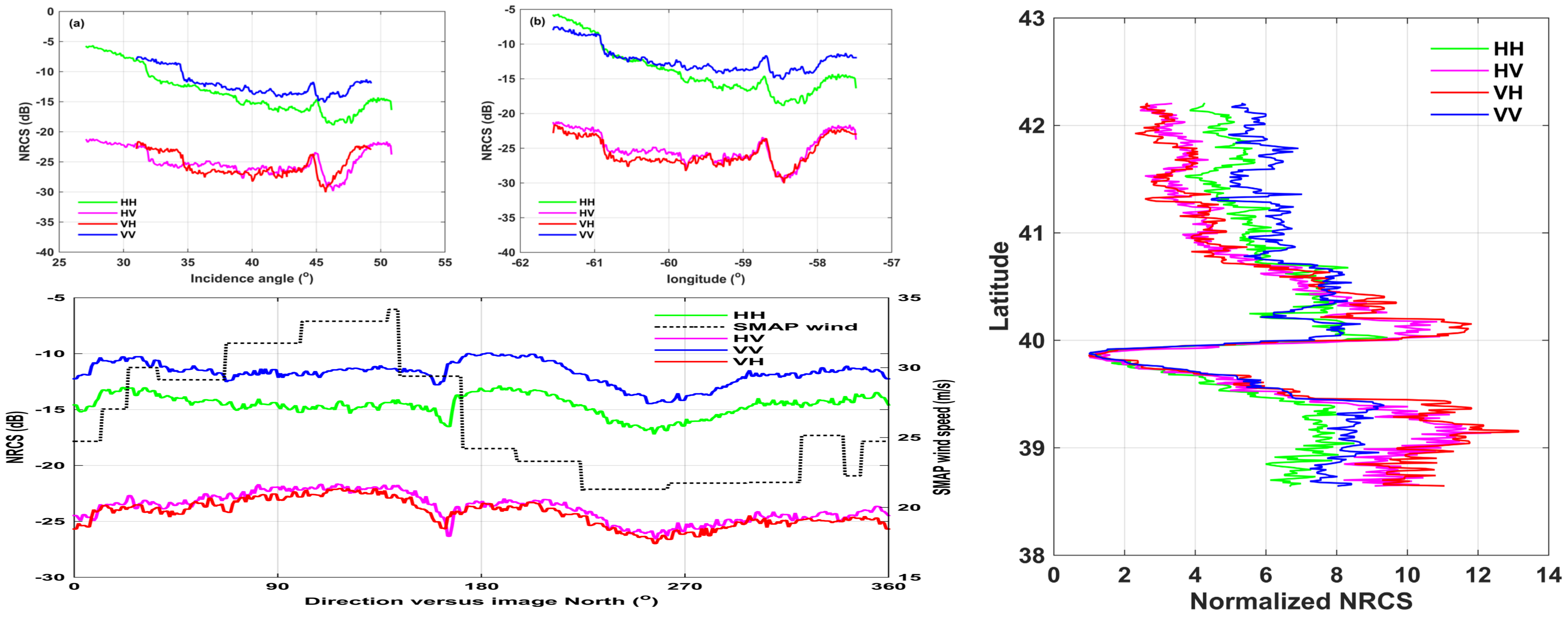

- For large incidence angles and high wind speeds, the sensitivity of HH-polarized NRCS to wind speed is higher than that of VV.

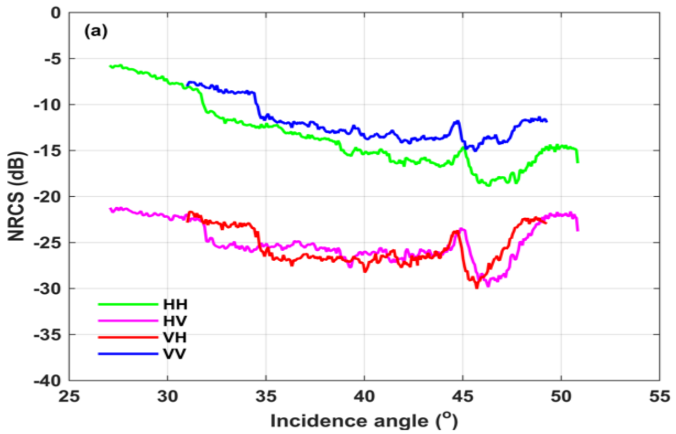

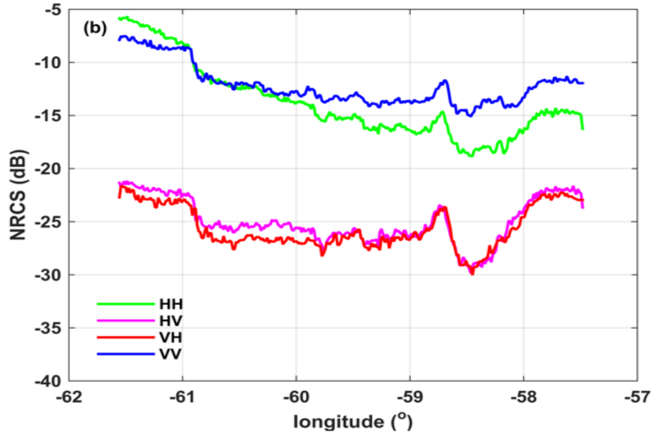

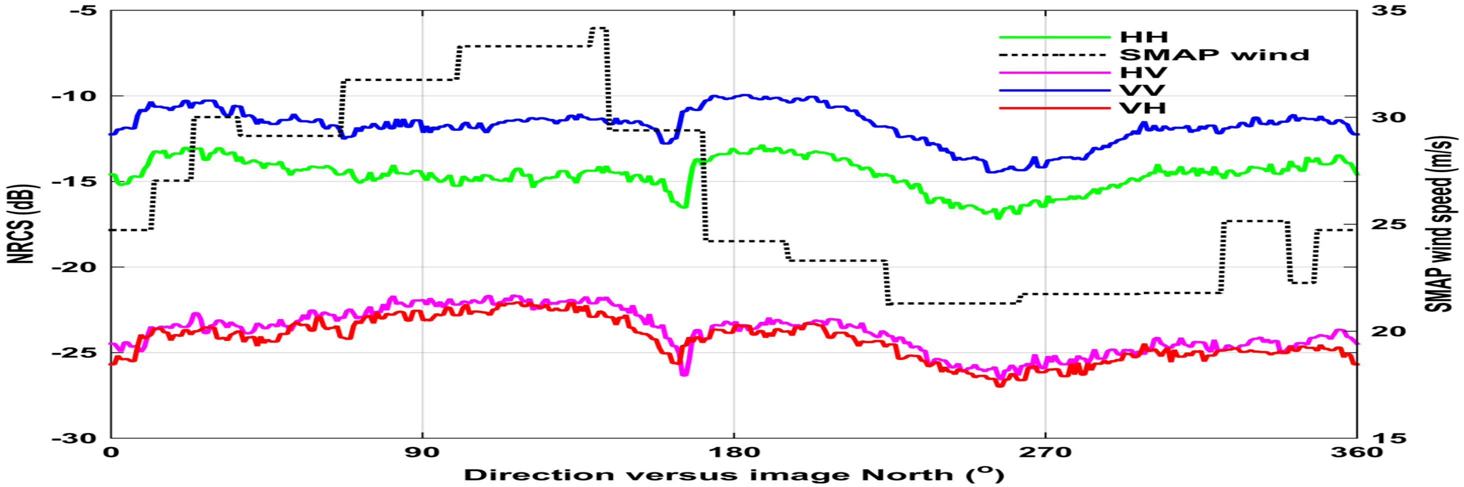

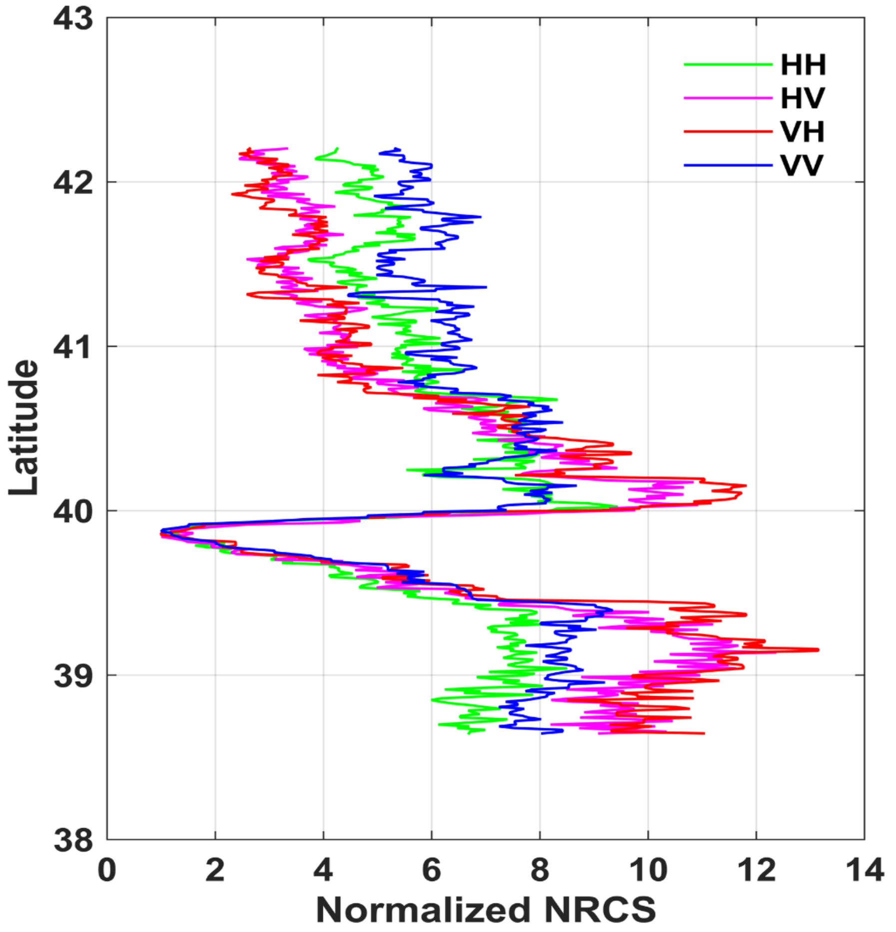

- Co- (VV, HH) and Cross-polarized (HV, VH) NRCSs gradually lose wind direction dependency at high winds.

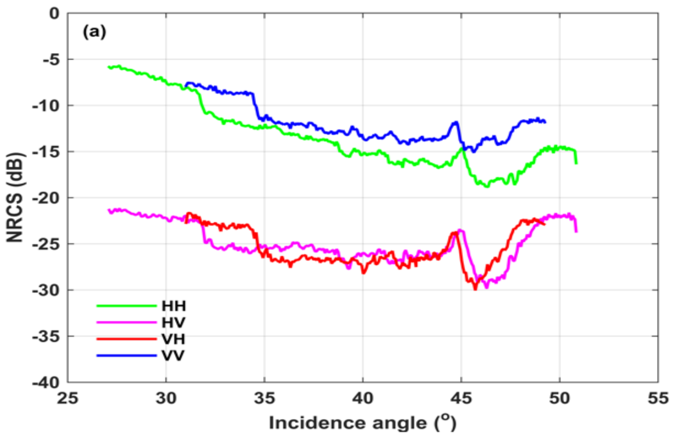

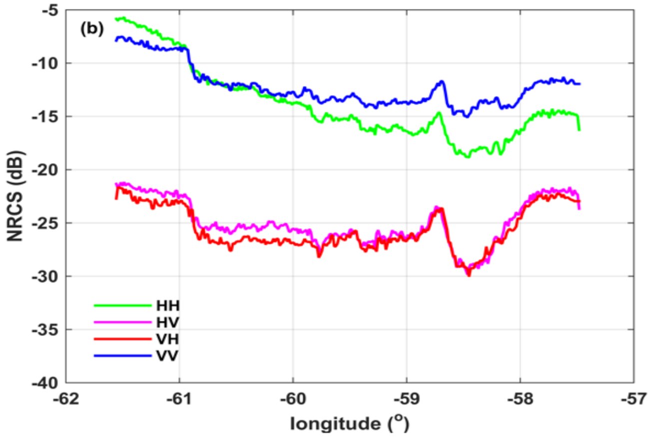

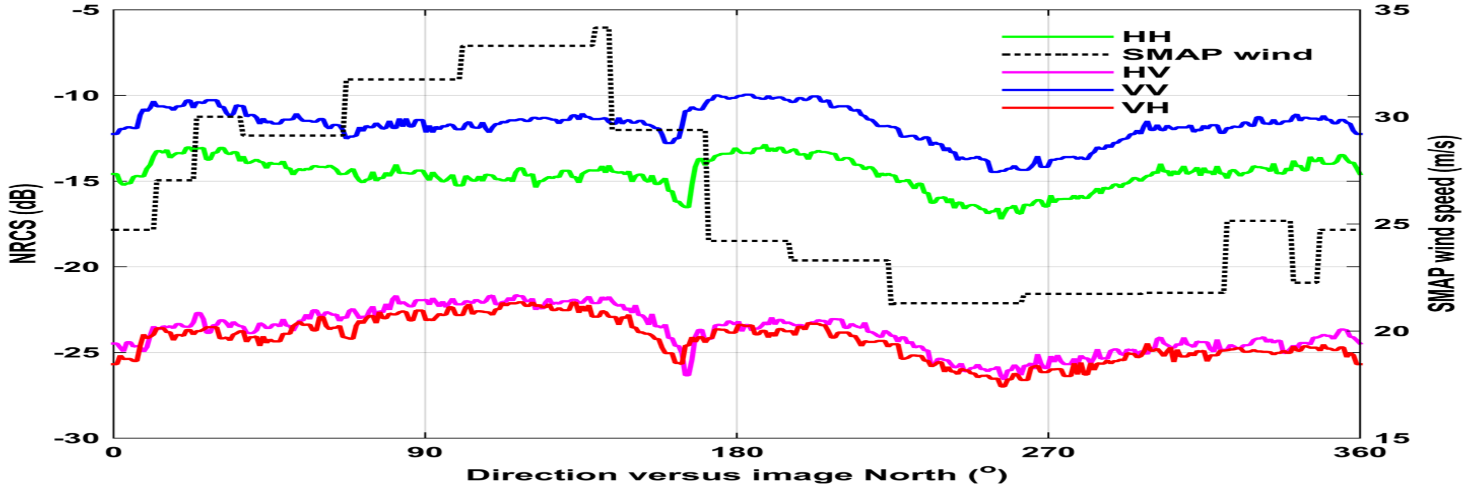

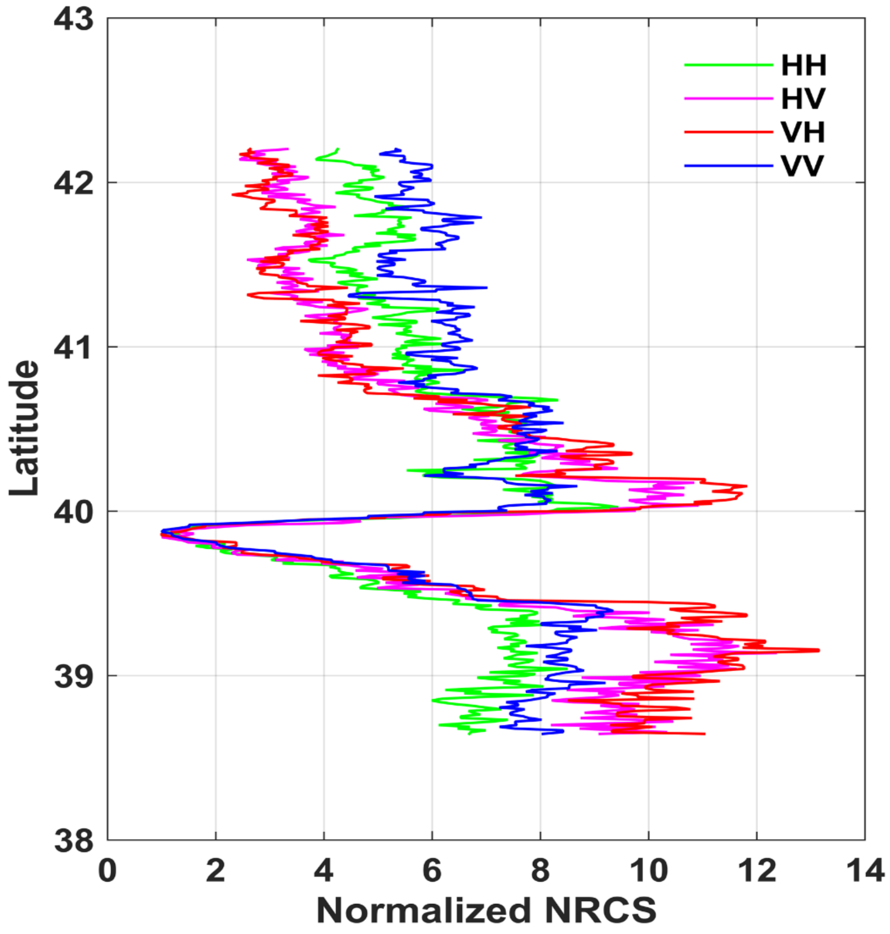

- Cross-polarization differences (HV-VH) within a short time interval have potential to reveal an asymmetric dynamic around the eye of Hurricane Epsilon.

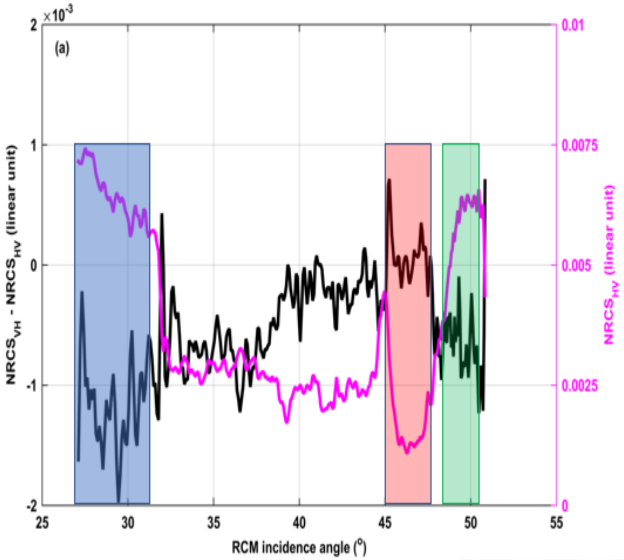

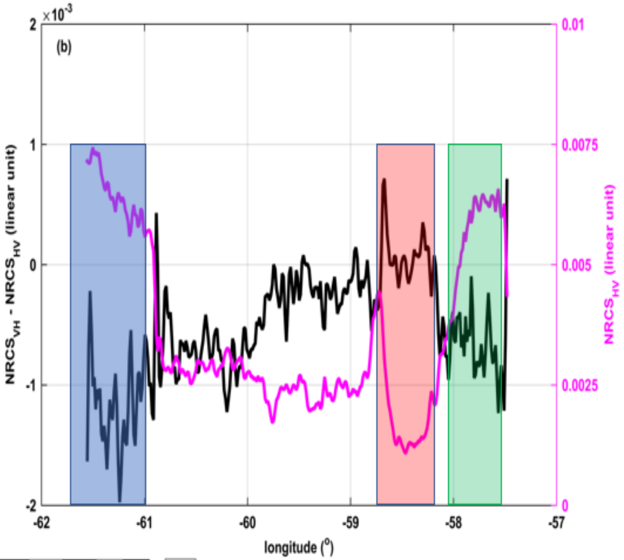

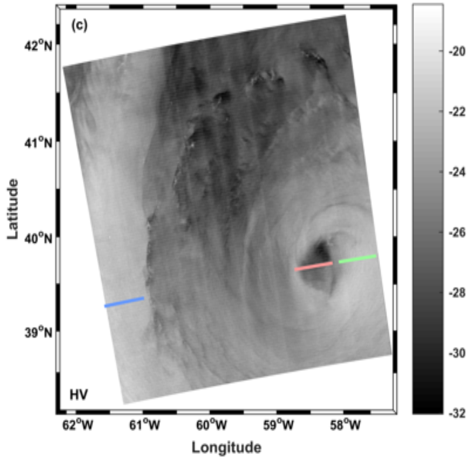

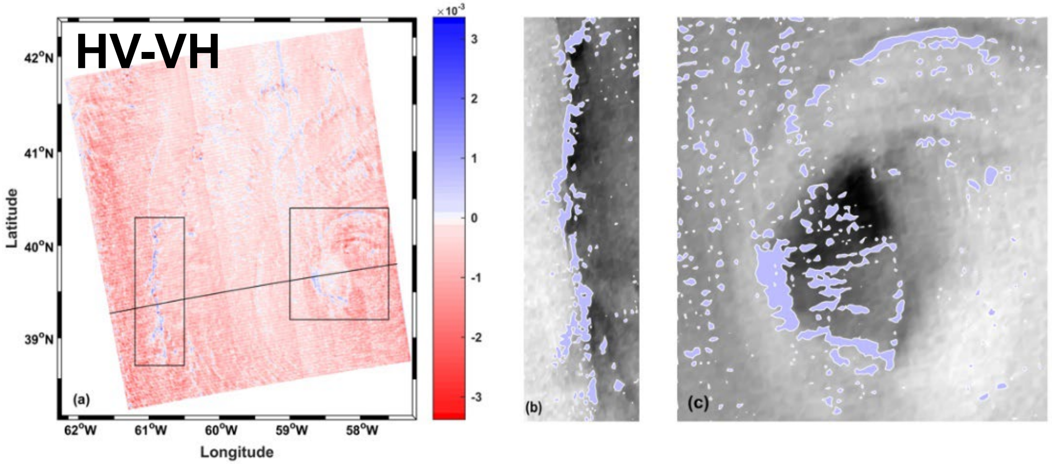

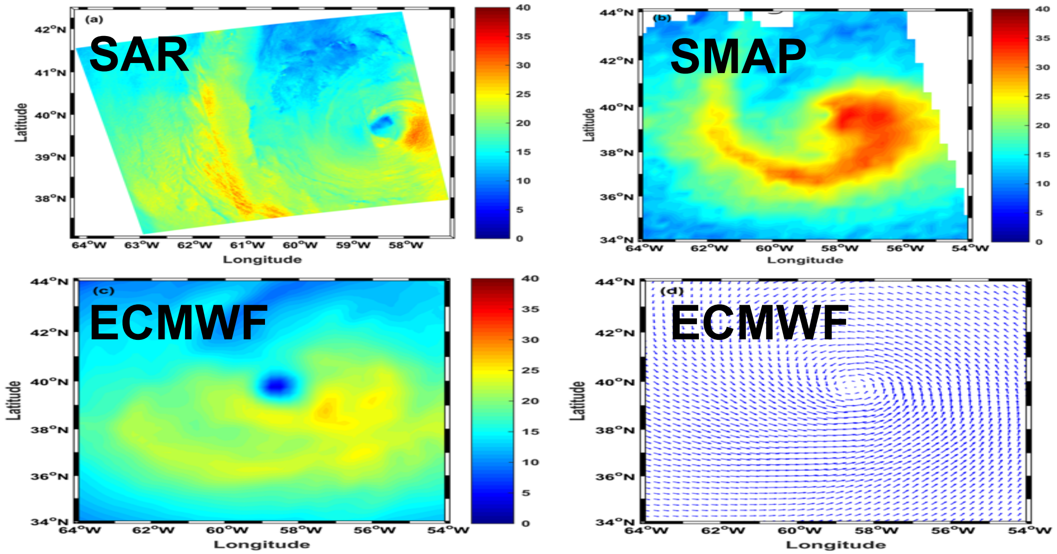

- Significant rain-induced NRCS attenuations are about 1.7 dB for HH and VV, and 2.2 dB for HV and VH, when the rain rate is 20 mm/h.

- These attenuations are associated with rain-induced turbulence and atmospheric absorption.

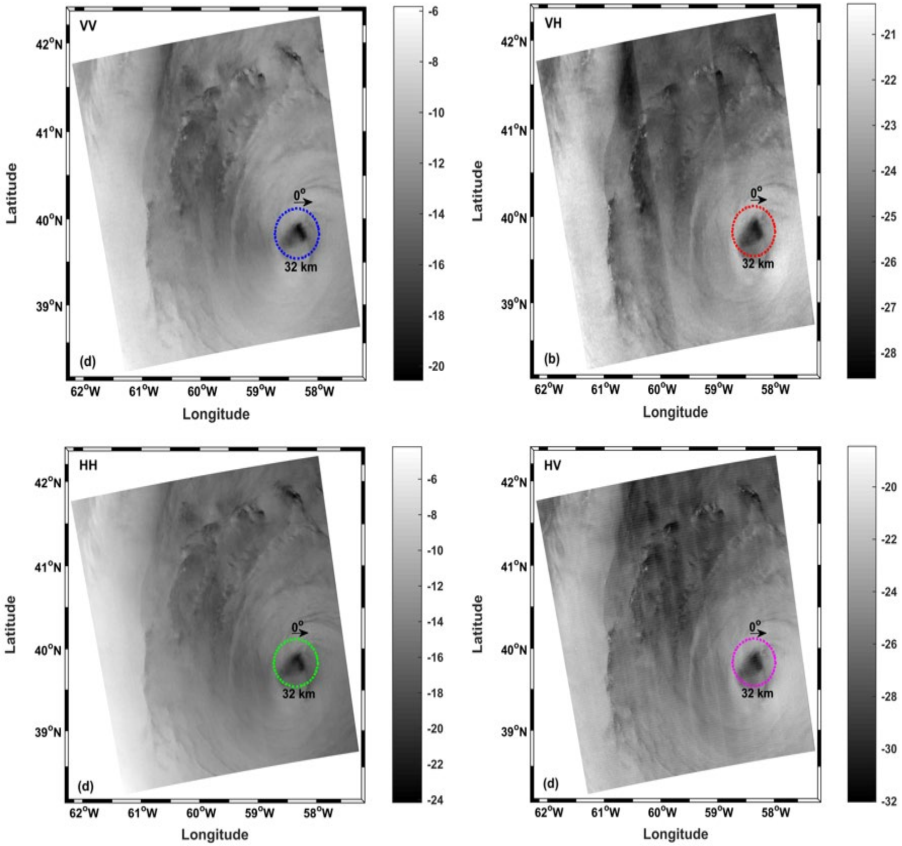

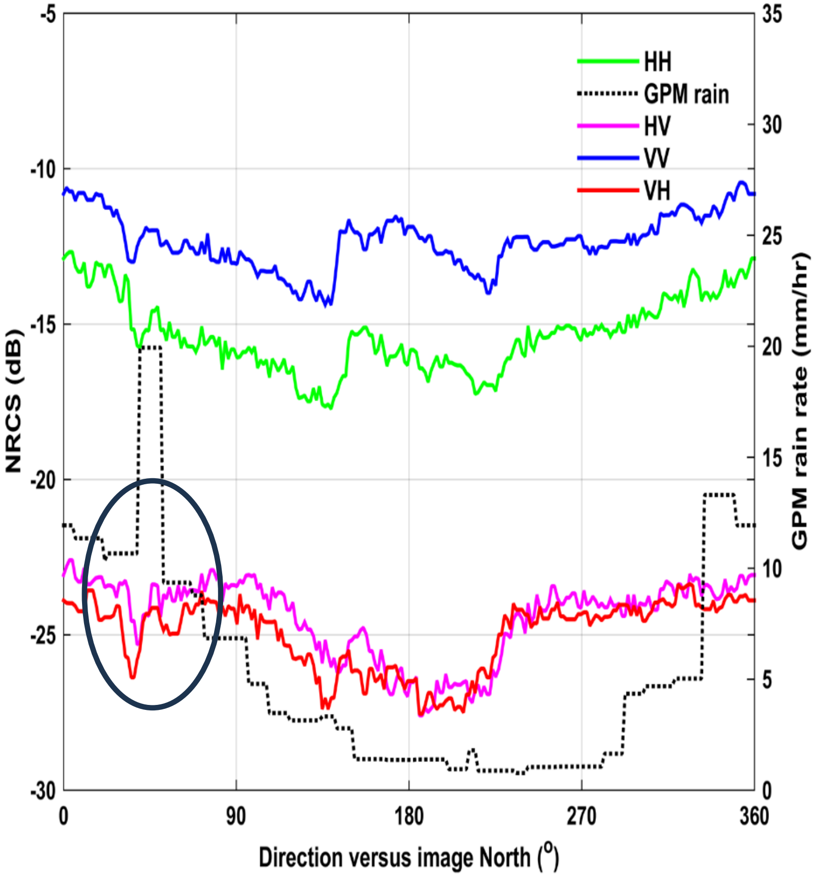

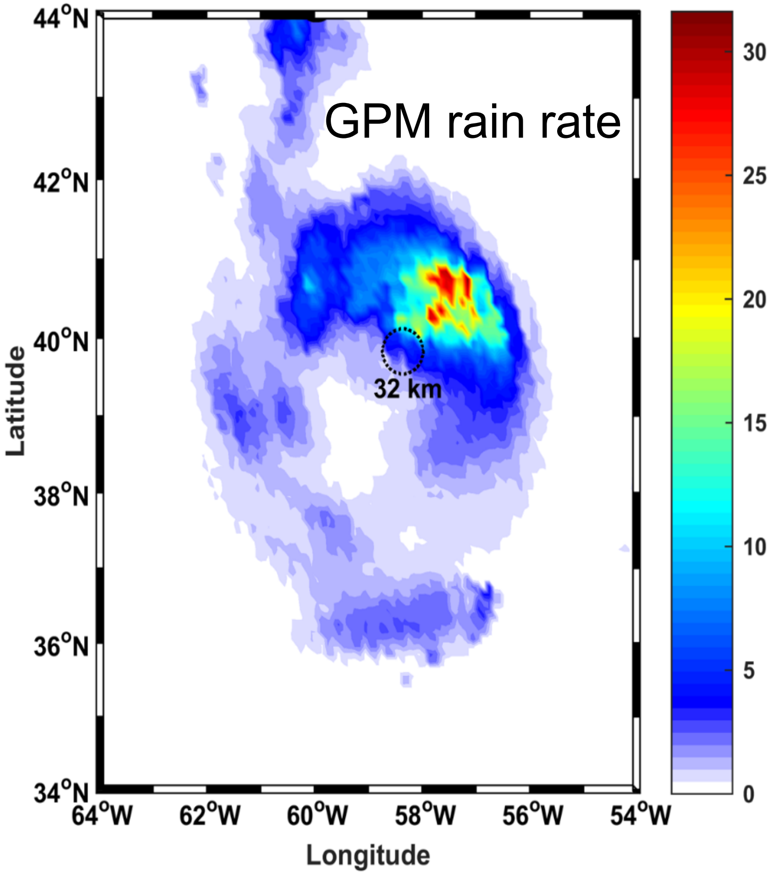

Tropical Cyclone Freddy

- Longest lifecycle: 37 days (5 February ~ 14 March)
- Category 5-equivalent tropical cyclone

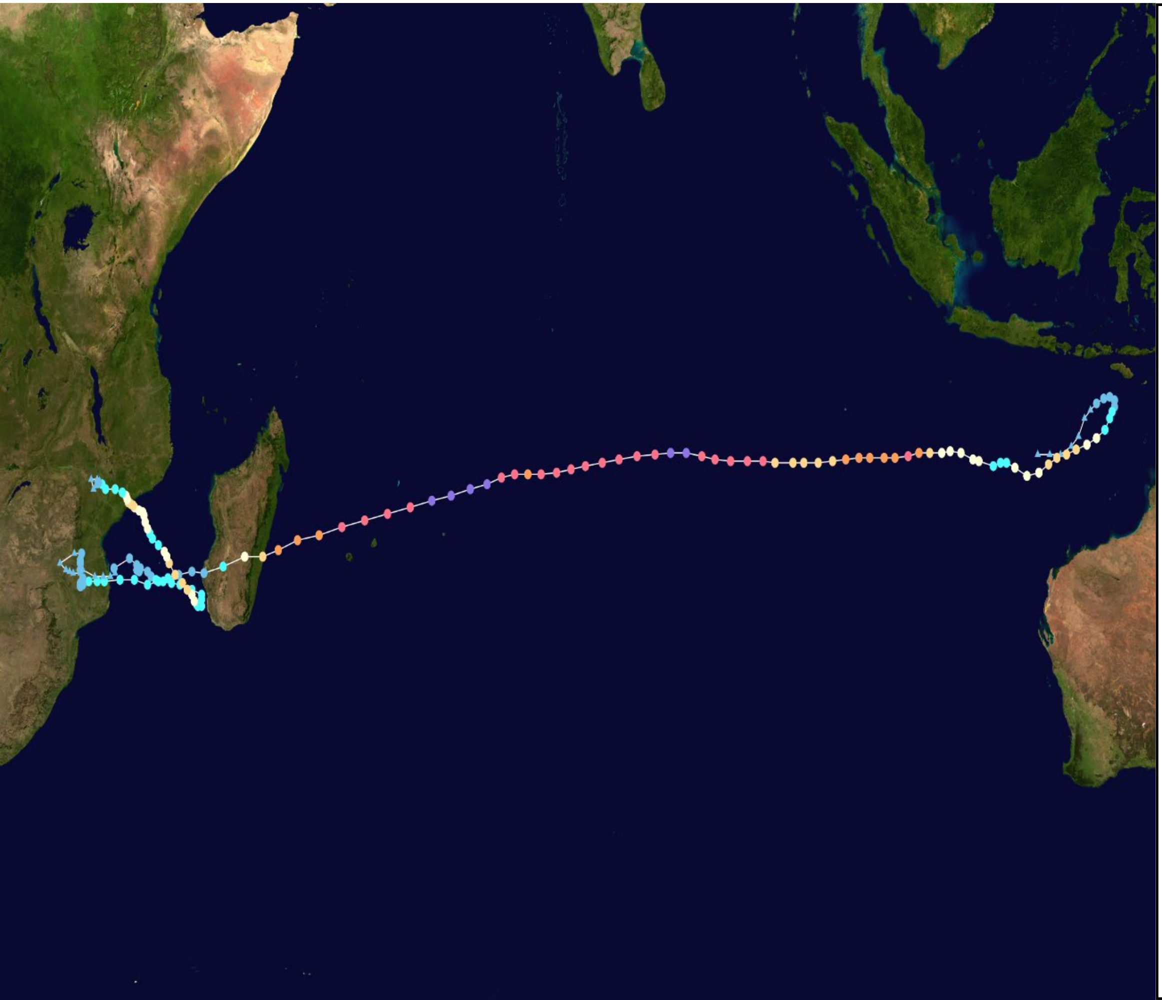

- 31 images were acquired by RCM, RADARSAT-2, and Sentinel-1.
- SAR constellations significantly increase temporal resolution, enabling the monitoring of the evolution of intensity and structure of TCs.

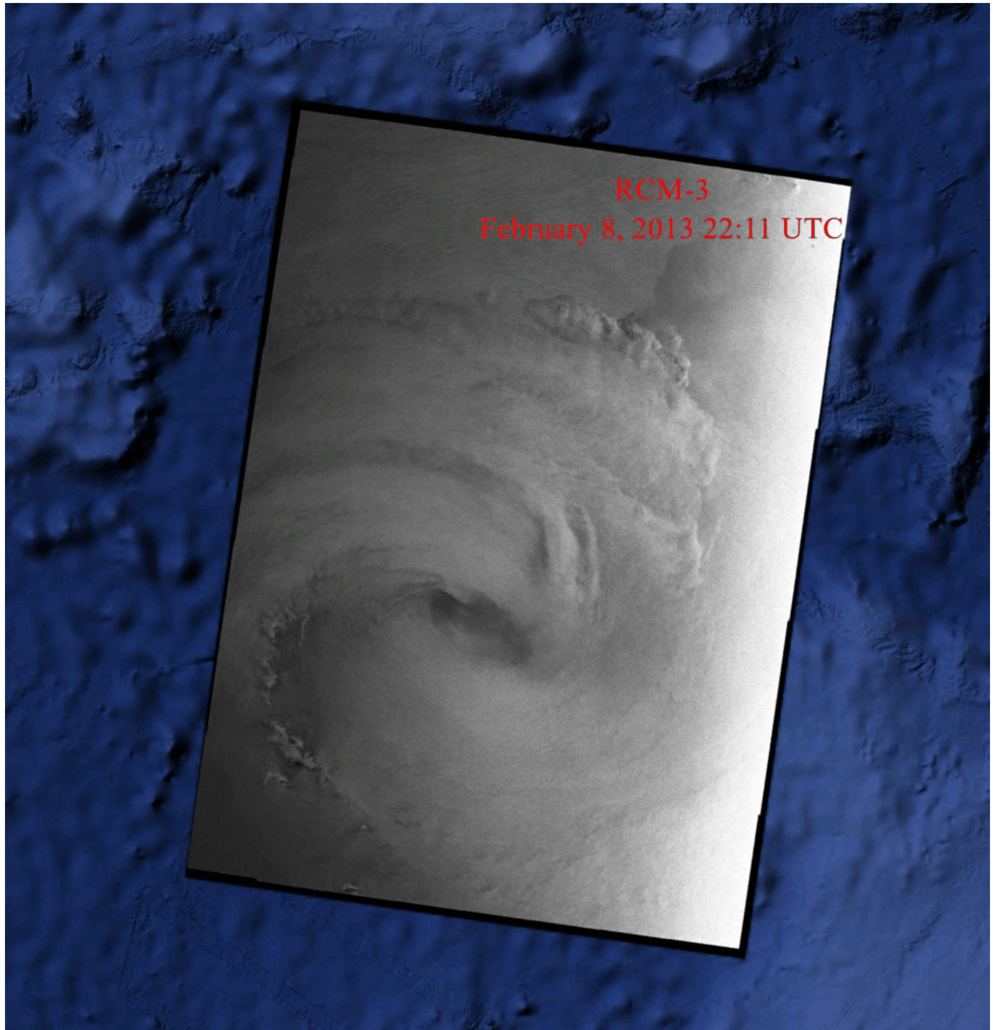

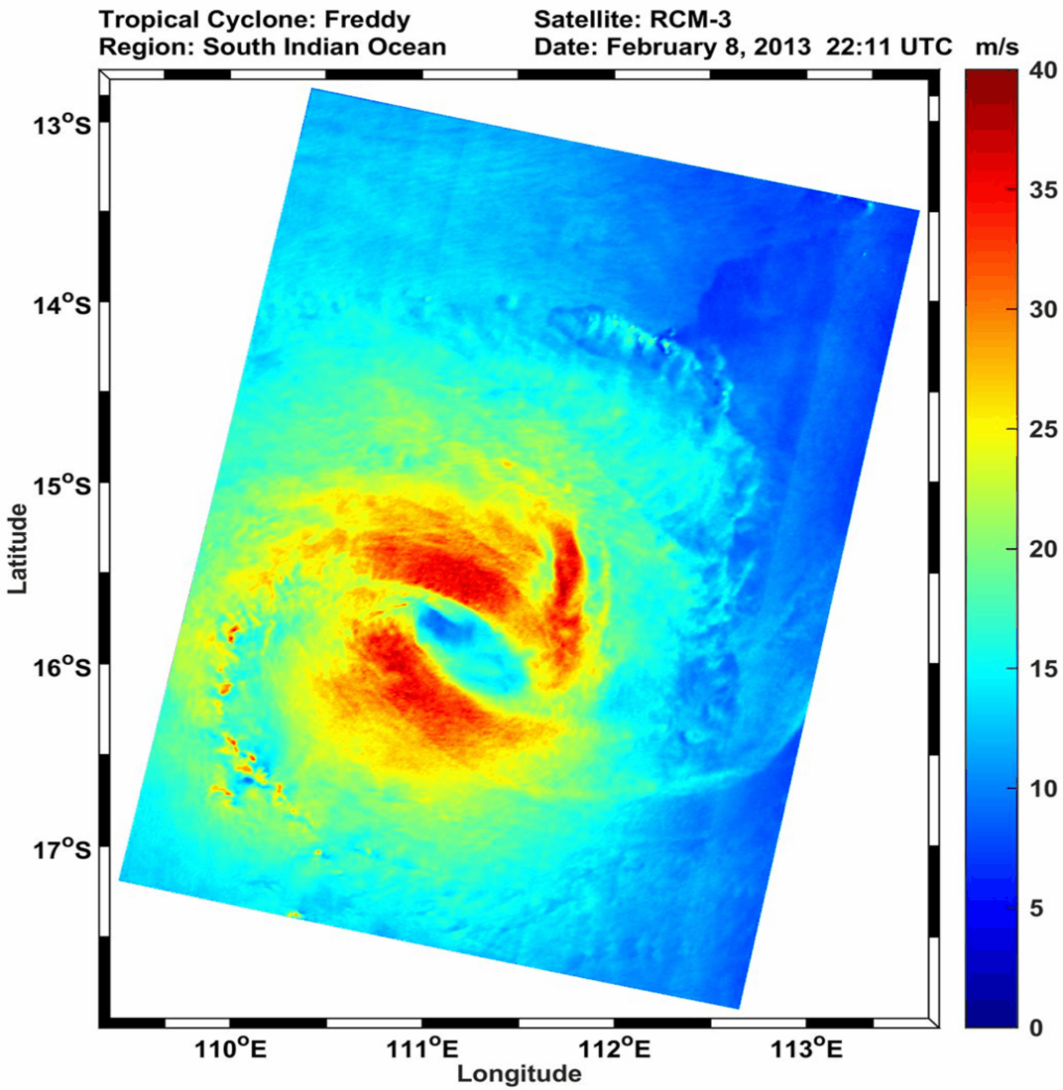

- TC intensity (Vmax) and structural parameters (34-, 50-, and 64-kt wind radii) are both estimated using wind fields from SAR and radiometer.

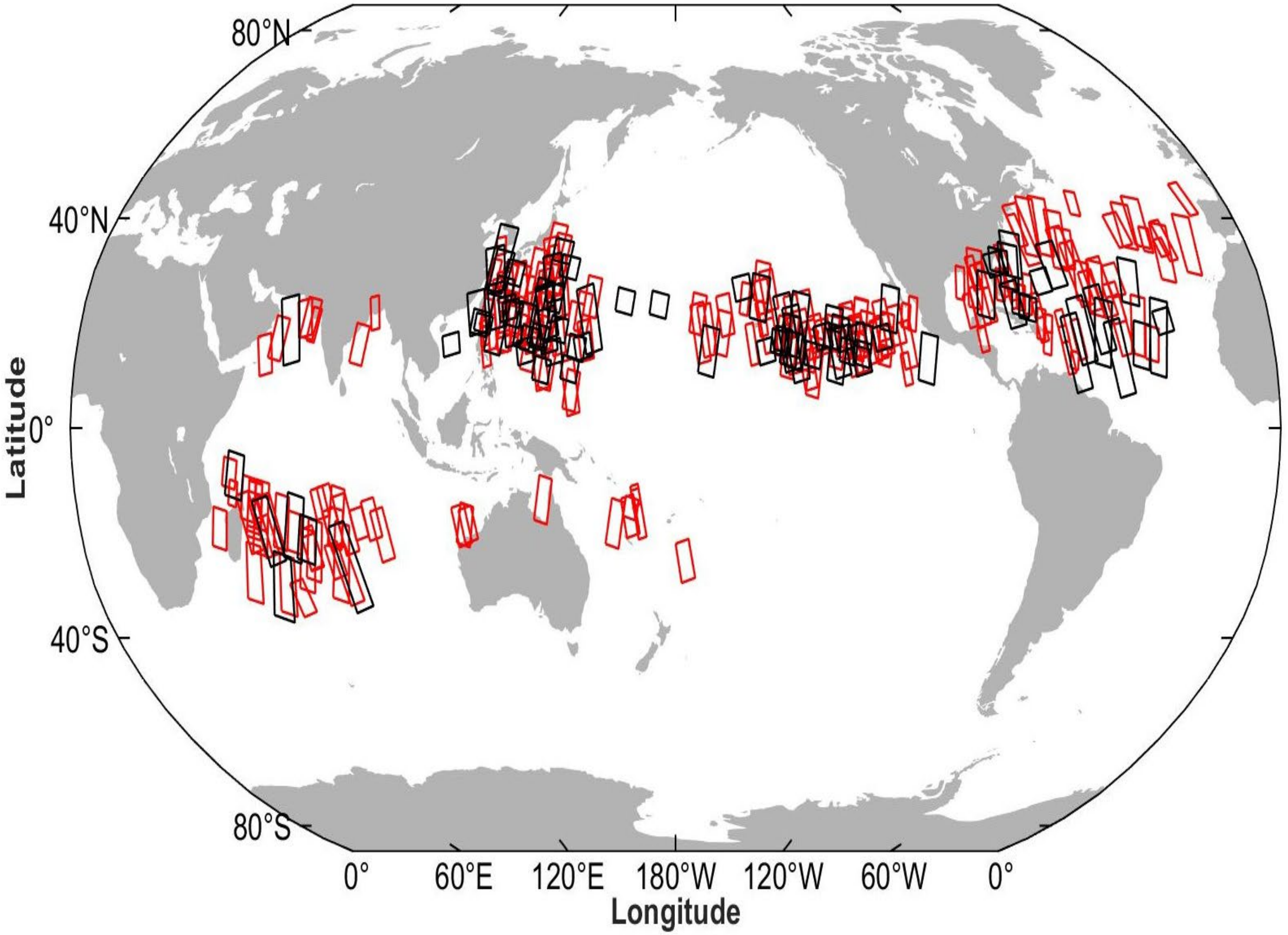

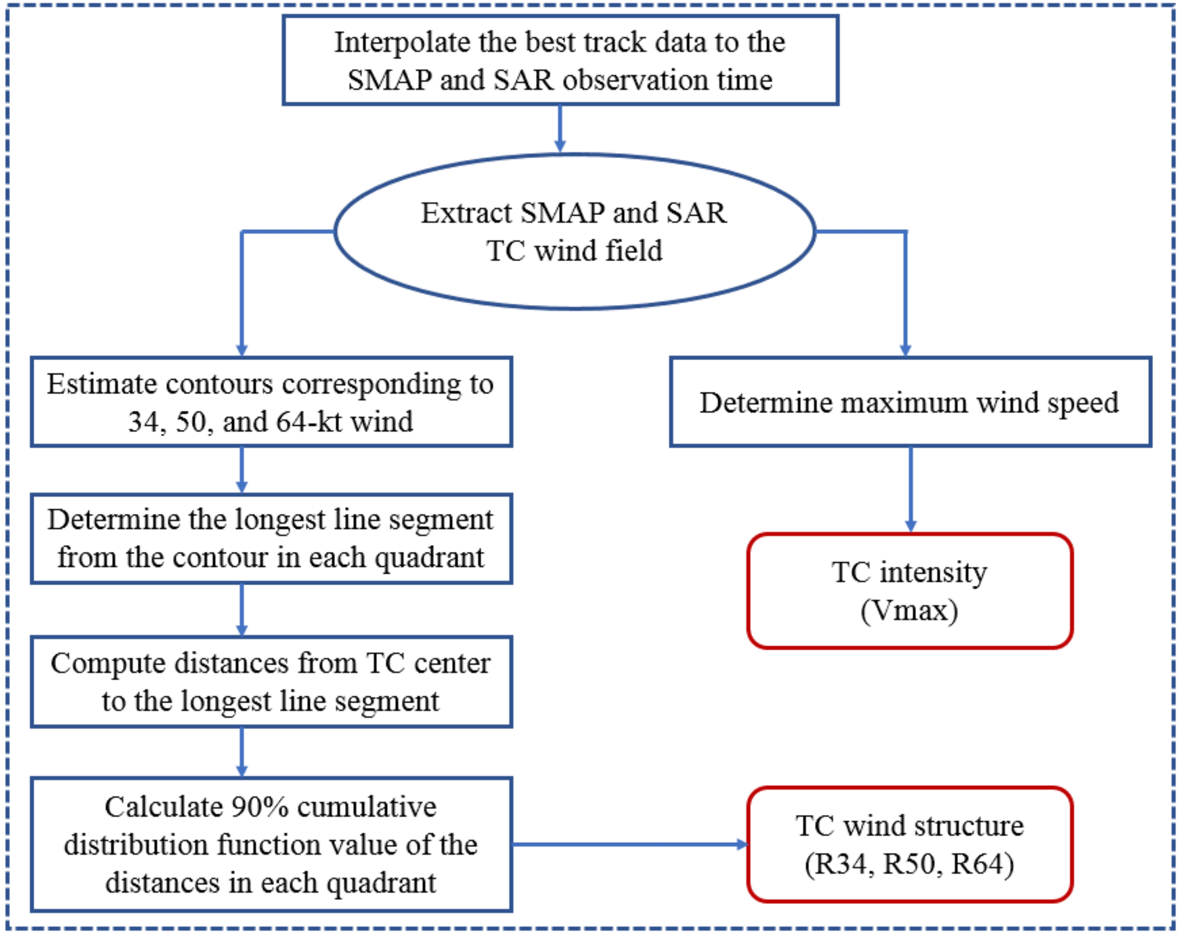

- A combination of the radiometer an SAR wind data acquired within a very short time interval has the potential to simultaneously obtain reasonable measurements of the wind radii and intensity parameters.

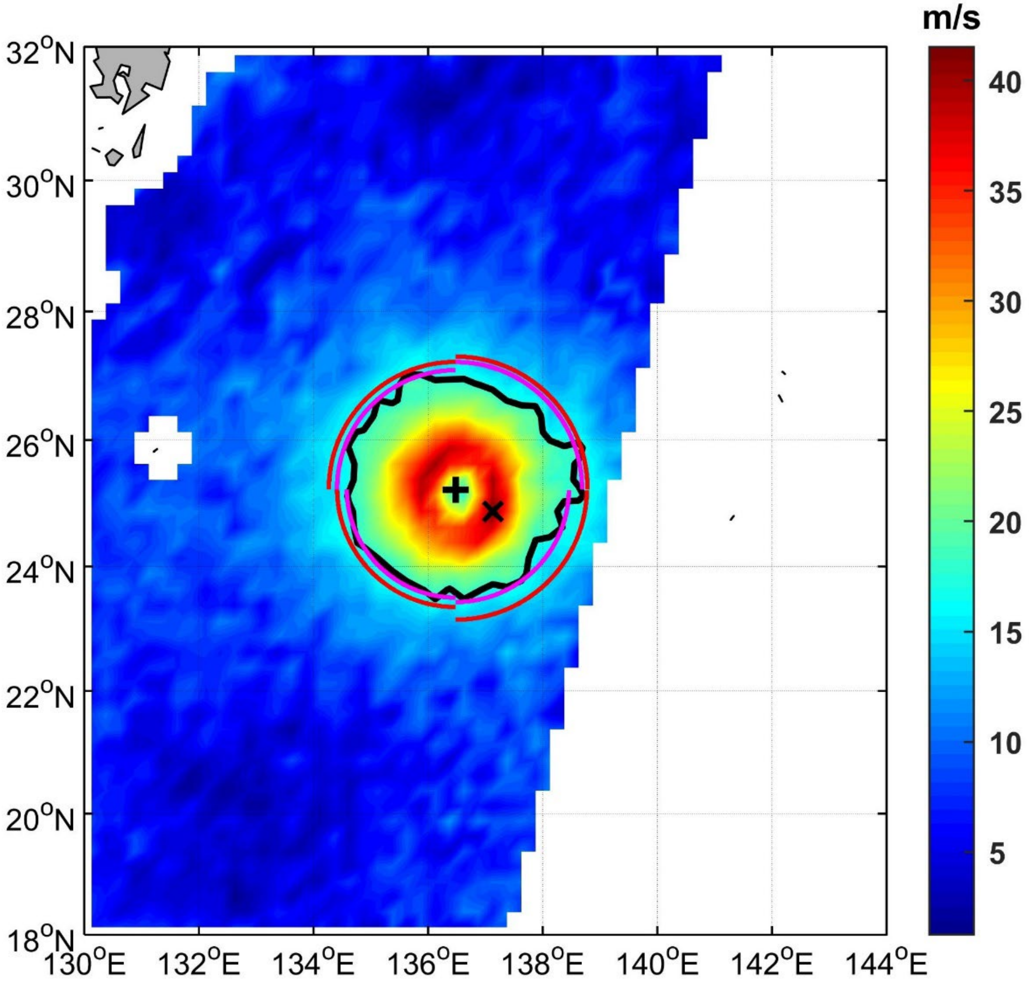

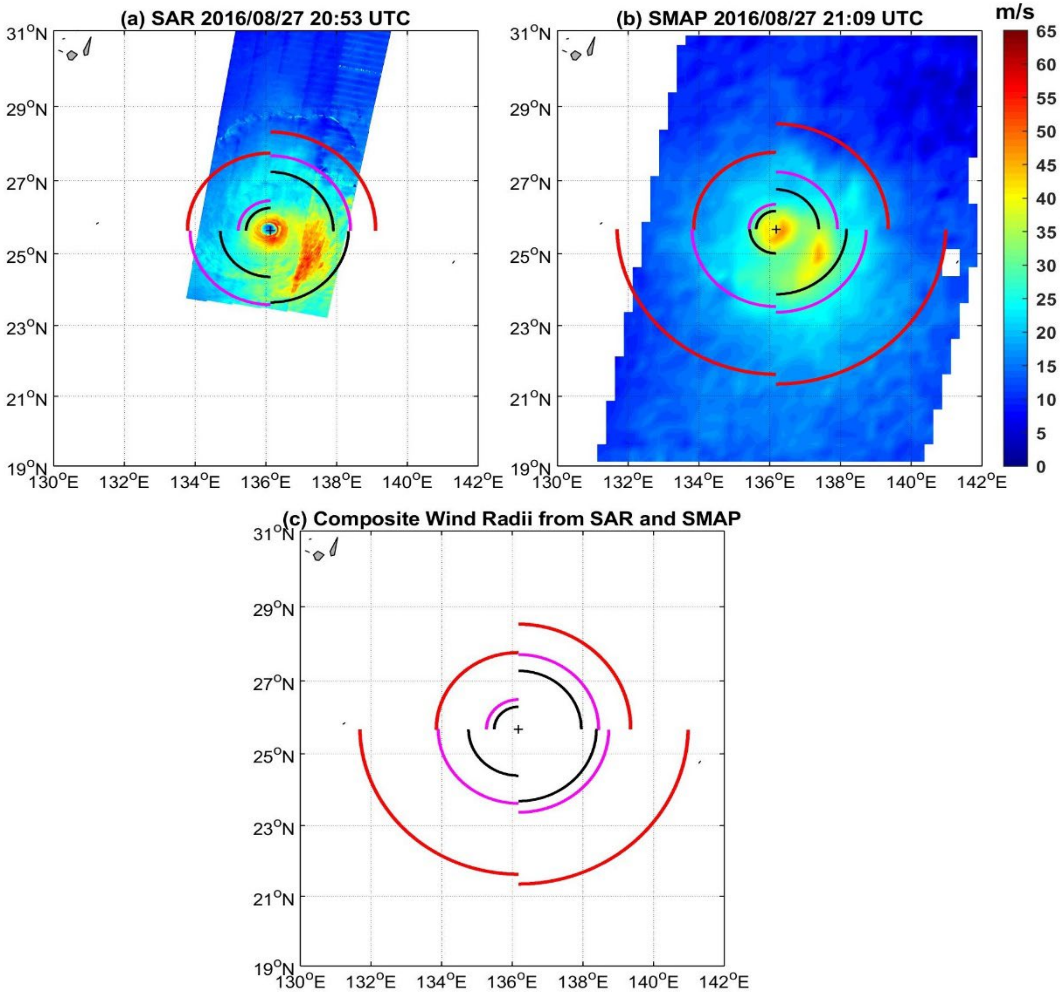

- The high-resolution and multitemporal synergistic observations from SAR and radiometer are valuable for studying fine-scale features of the wind field and characteristics of wind asymmetry associated with intensity change, as well as the evolution of TC surface wind structure and intensity.

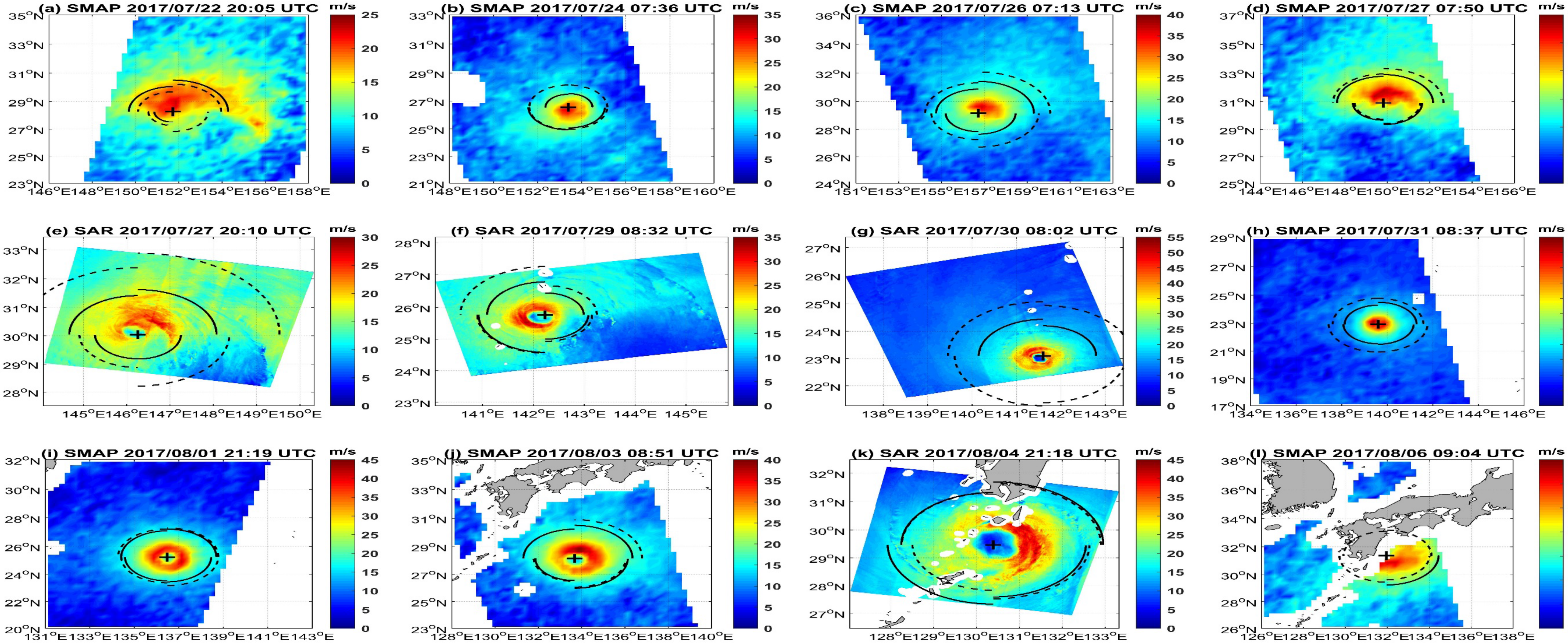

Zhang et al. 2021, IEEE JSTARS

- The tracks and translation velocities of TCs can be determined from multi-temporal SAR images.

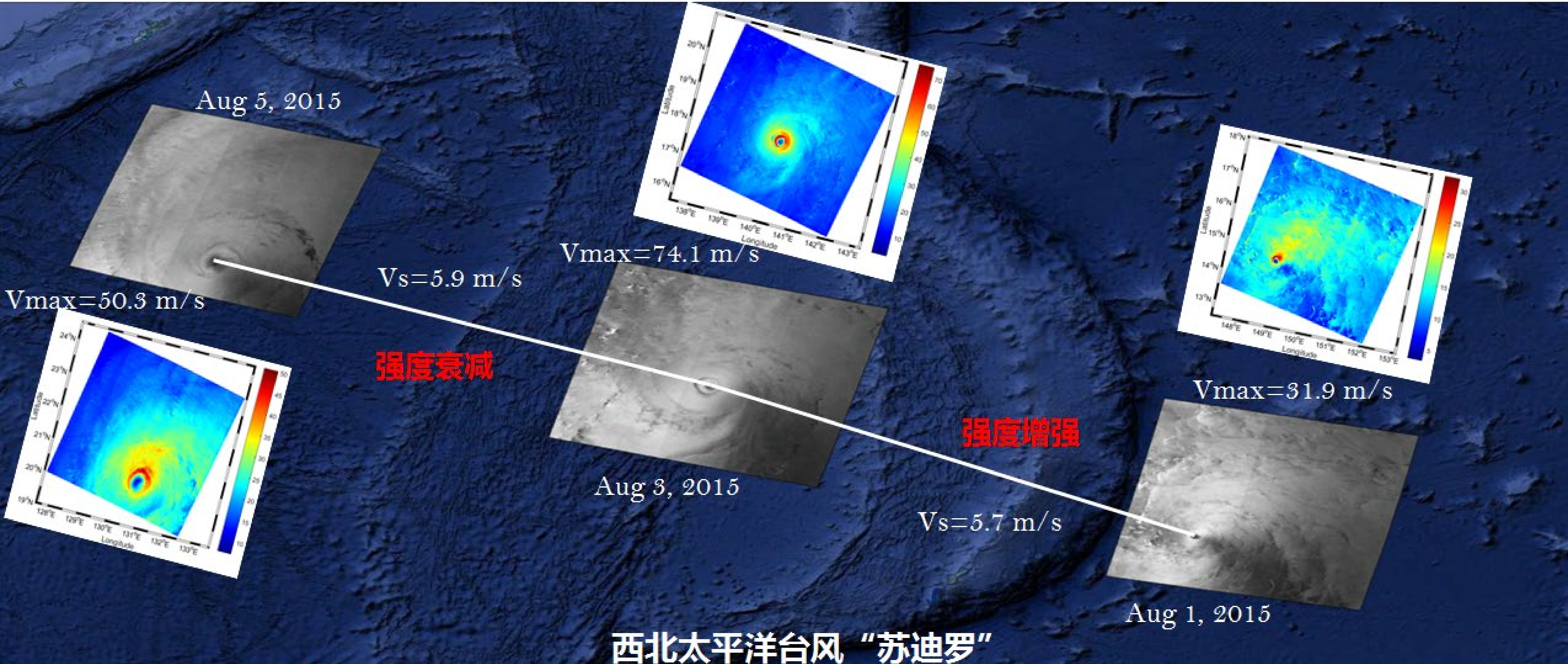

- We develop long time-series of tropical cyclone wind field and structure parameter products.

SAR： Sentinel-1、RADARSAT-2、RCM

Resolution： 1 km

Period： 2008-2023

Format： NETCDF

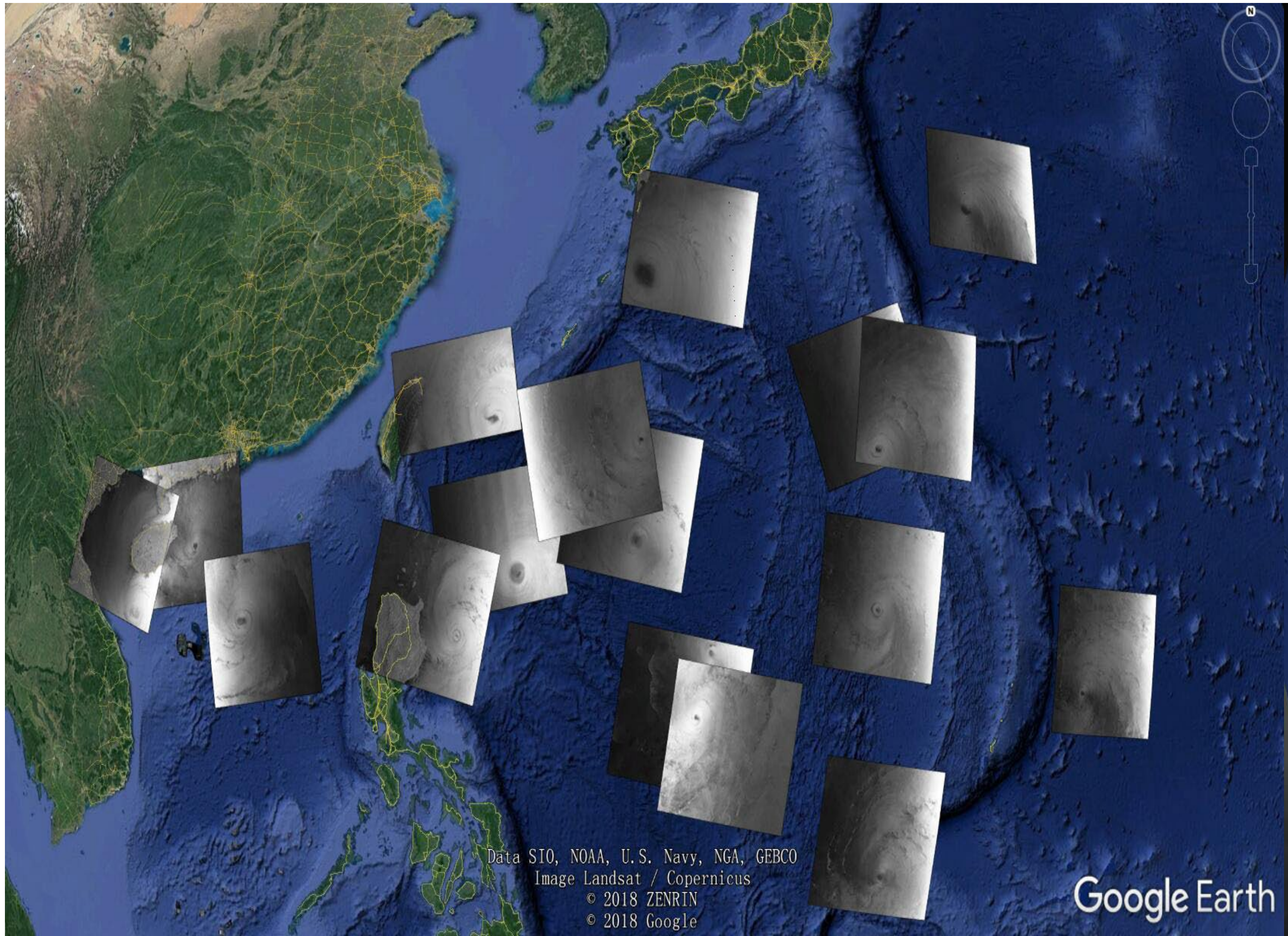

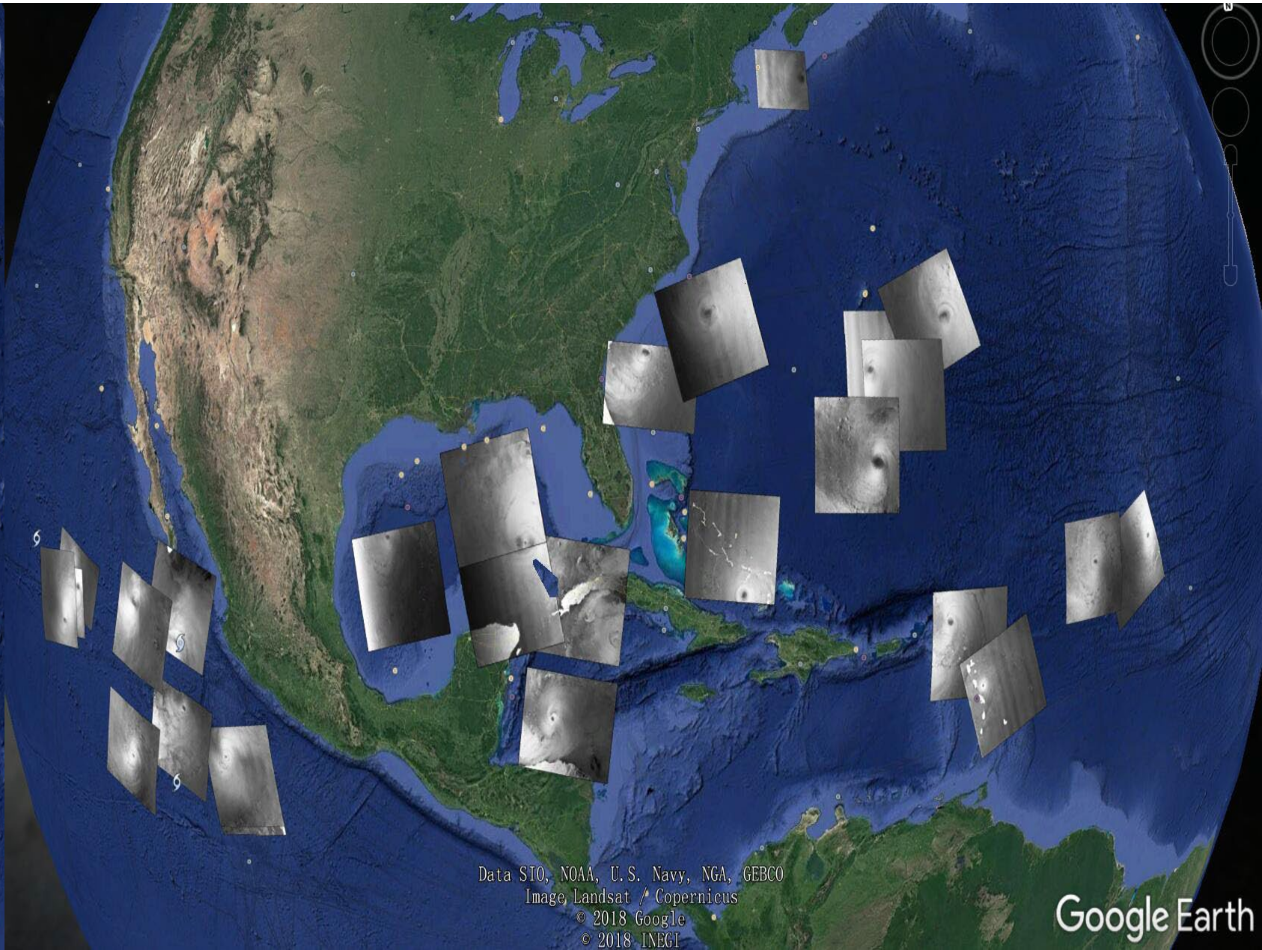

sextant.ifremer.fr/geonetwork/srv/eng/catalog.search#/metadata/447aa88f-0c0b-4607-afe2-9c77e95a14b8

High Resolution Tropical Cyclone Vortex and Wind Structure from SAR Imagery for ESA MAXSS Project

View | Back

Version 1.0 | DOI 10.12770/447aa88f-0c0b-4607-afe2-9c77e95a14b8 | Status Completed

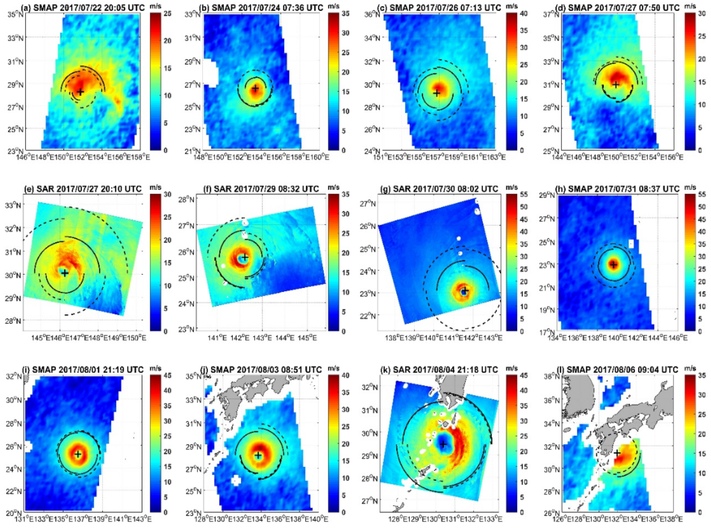

The main objective of this dataset is to gather the ocean surface wind fields measured by two C-band synthetic aperture radar (SAR) satellites (e.g, RADARSAT-2 and Sentinel-1) under extreme weather conditions. This dataset aims at providing high-resolution tropical cyclone (TC) ocean surface wind speeds, directions, 34-, 50-, and 64-kt wind radii in each geographical quadrant.

TC ocean surface wind speeds and directions were retrieved from RADARSAT-2 and Sentinel-1 dual-polarization (VV, VH) SAR imagery, based on the Bayesian method and local gradient approach, respectively. The procedure for estimating wind radii can be summarized as three steps. First, the contours of each wind radii are computed, which consists of a number of line segments. Then, the distances from the storm center to each point of the longest line segment in each quadrant are calculated. Finally, the 90% cumulative distribution of this distance is defined as the wind radii of a given wind threshold at that quadrant. The SAR-retrieved high-resolution TC ocean surface wind fields and add-values (e.g., 34-, 50-, and 64-kt wind radii) haven been validated using observations from buoys, airborne stepped-frequency microwave radiometer, GPS dropsonde, and spaceborne radiometers.

This dataset was produced in the frame of the ESA funded Marine Atmosphere eXtreme Satellite Synergy (MAXSS) project. The primary objective of the ESA Marine Atmosphere eXtreme Satellite Synergy (MAXSS) project is to provide guidance and innovative methodologies to maximize the synergetic use of available Earth Observation data (satellite, in situ) to improve understanding about the multi-scale dynamical characteristics of extreme air-sea interaction.

Author(s) Zhang Biao (NUIST > Nanjing University of Information Science and Technology), William Perrie (BIO > Bedford Institute of Oceanography)

Publication date 2023-03-30

ID: MAXSS-L4-WAVE-TCVORTEX

Project(s) MAXSS

Product

Level L4
Latency Historical

Observation source(s)

Sentinel-1 A / C-band SAR, Sentinel-1 B / C-band SAR, RADARSAT-2 / SAR

Temporal

Temporal properties 01-09-2012 → 30-11-2021
Resolution

Spatial

Geographic area Global
Resolution 1 km
Projection WGS 84 (EPSG:4326)
Bounding box Latitude -40.00 to 40.00, Longitude -180.00 to 180.00

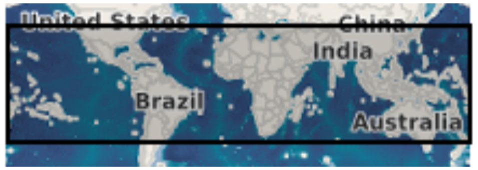

Zhang & Perrie, 2023

- Wave gliders can simultaneously observe surface winds and currents in the TC cores， but only provide measurements along the glider tracks.

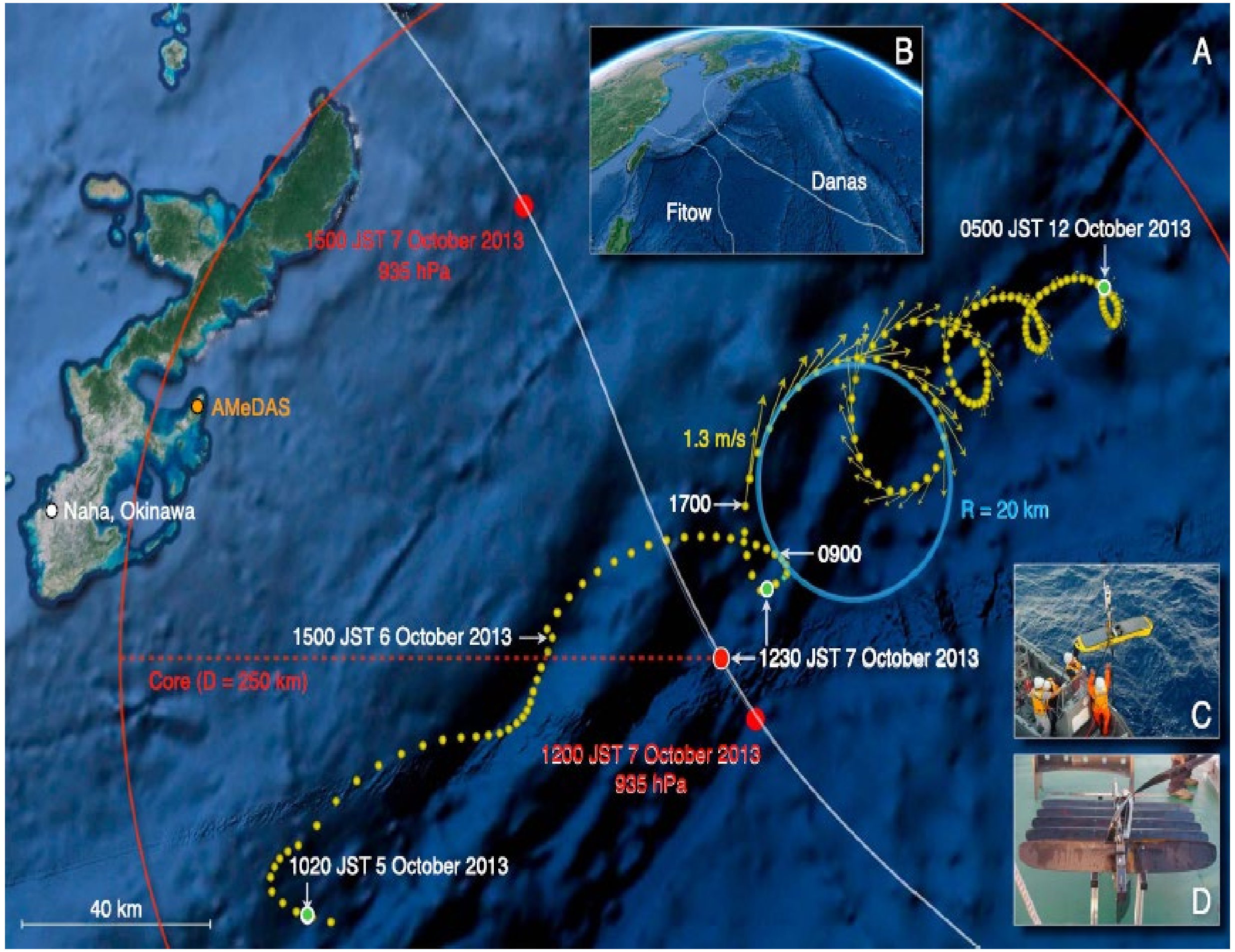

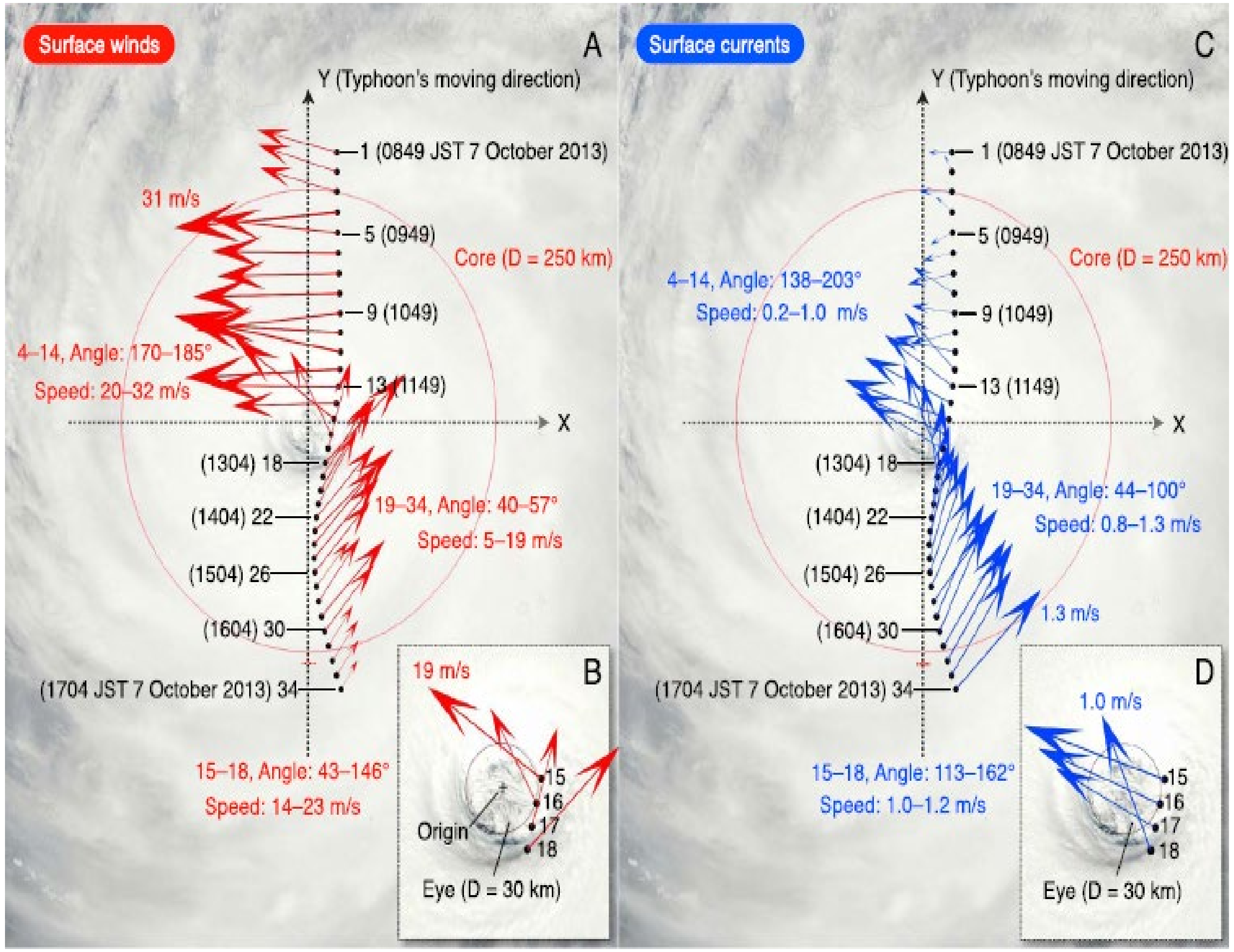

Mitarai & McWilliams, 2016

- The collocations between near-surface currents from drifting buoys and wind fields from multi-mission satellites (SAR, radiometer, and scatterometer) provide an unique opportunity to investigate winds and currents under extreme weather conditions.

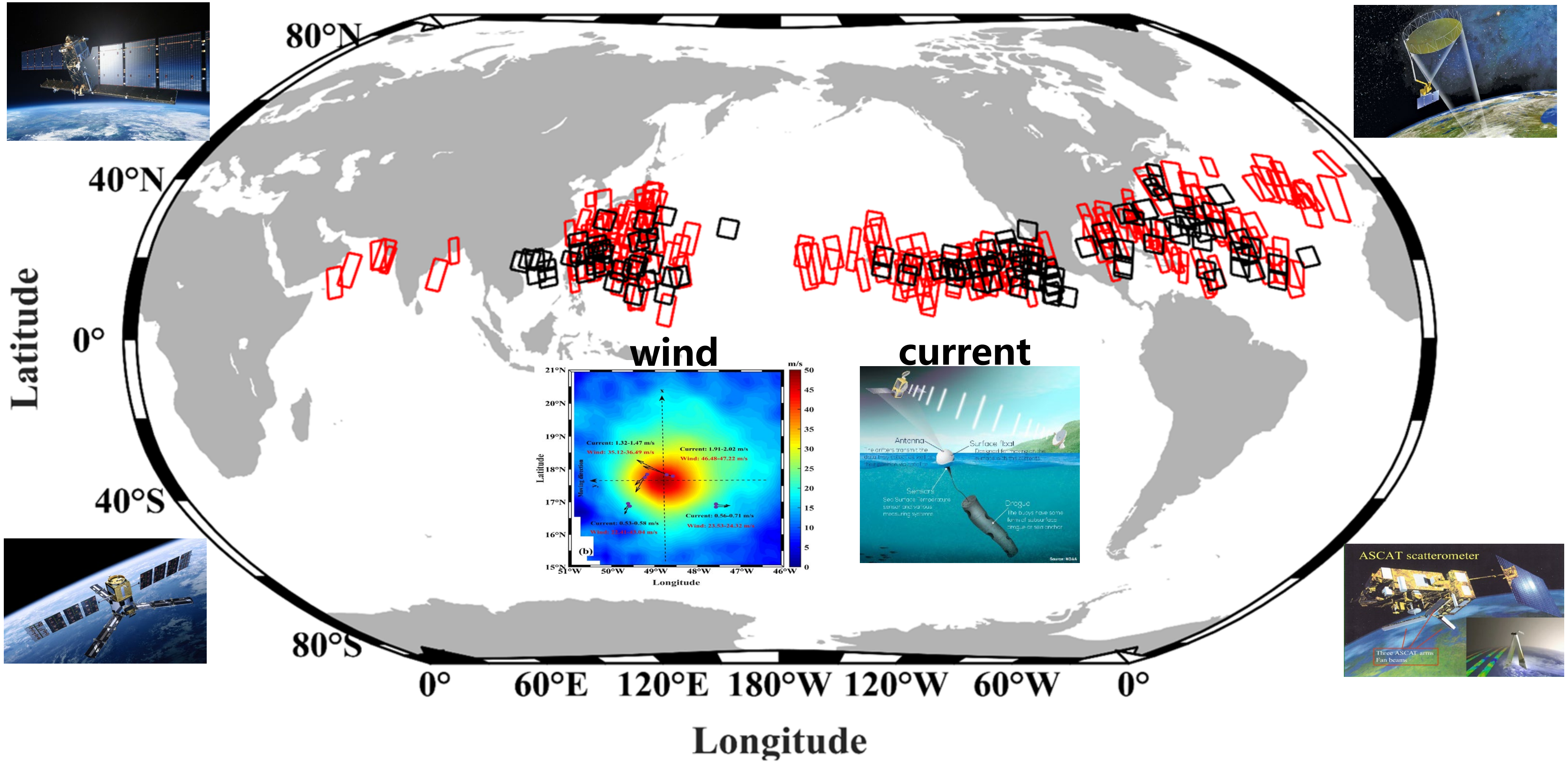

long time-series of wind fields from multi-mission satellites

2007~2022

Satellite	Payload	Frequency	Resolution
RADARSAT-2	SAR	C	1×1 km
Sentinel-1A/B	SAR	C	1×1 km
SMAP	radiometer	L	25×25 km
SMOS	radiometer	L	25×25 km
ASCAT	scatterometer	L	25×25 km

near-surface currents from drifters

	Depth	Resolution	Resource
drifter	15 m	1 hour	Global Drifter Program (GDP)

- Observed near-surface current speeds increase linearly with wind speeds in the four tropical cyclone quadrants.

The depth of mixed layer for fast-moving TCs： $h \sim U_{10}[R_{max}/(NU_h)]^{1/2}$

Wind-driven current velocity in the mixed layer: $U_s \sim \tau\, R_{max}/(hU_h)$

$$\boldsymbol{U_s \sim U_{10}(N\, R_{max}/U_h)^{1/2}}$$

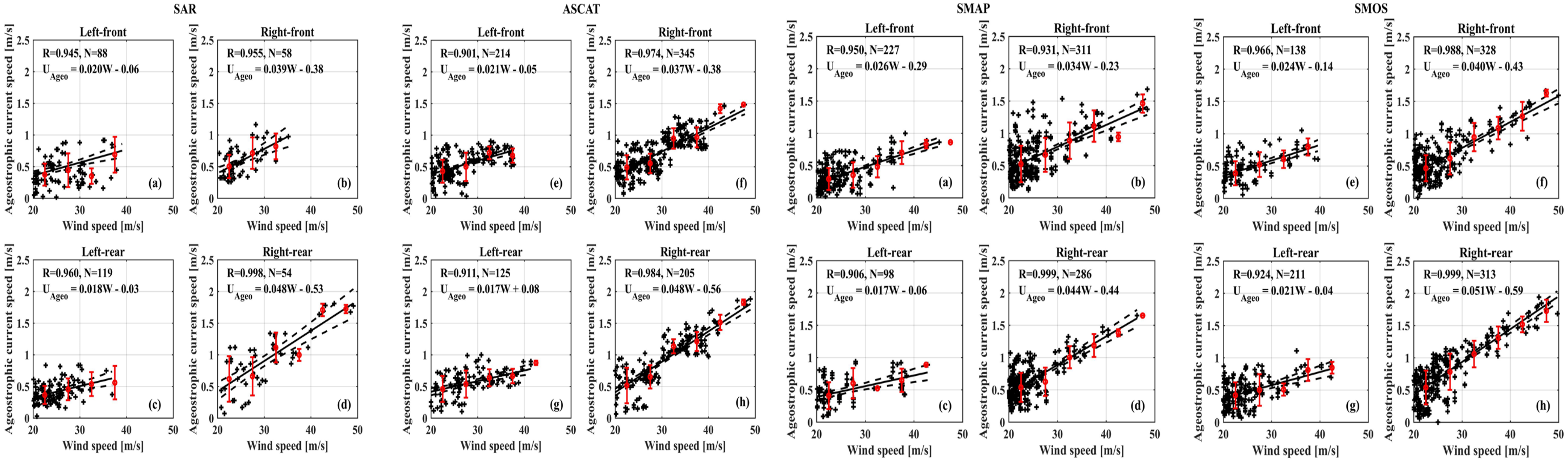

Fan & Zhang et al. 2022 JGR: Oceans

- Surface winds and currents both exhibit strong asymmetric features, with the largest wind speeds and currents on the TC right side.
- Wind directions are approximately aligned with current directions in the right-front quadrant; a difference of about 90° occurs in the left-front and left-rear quadrants/

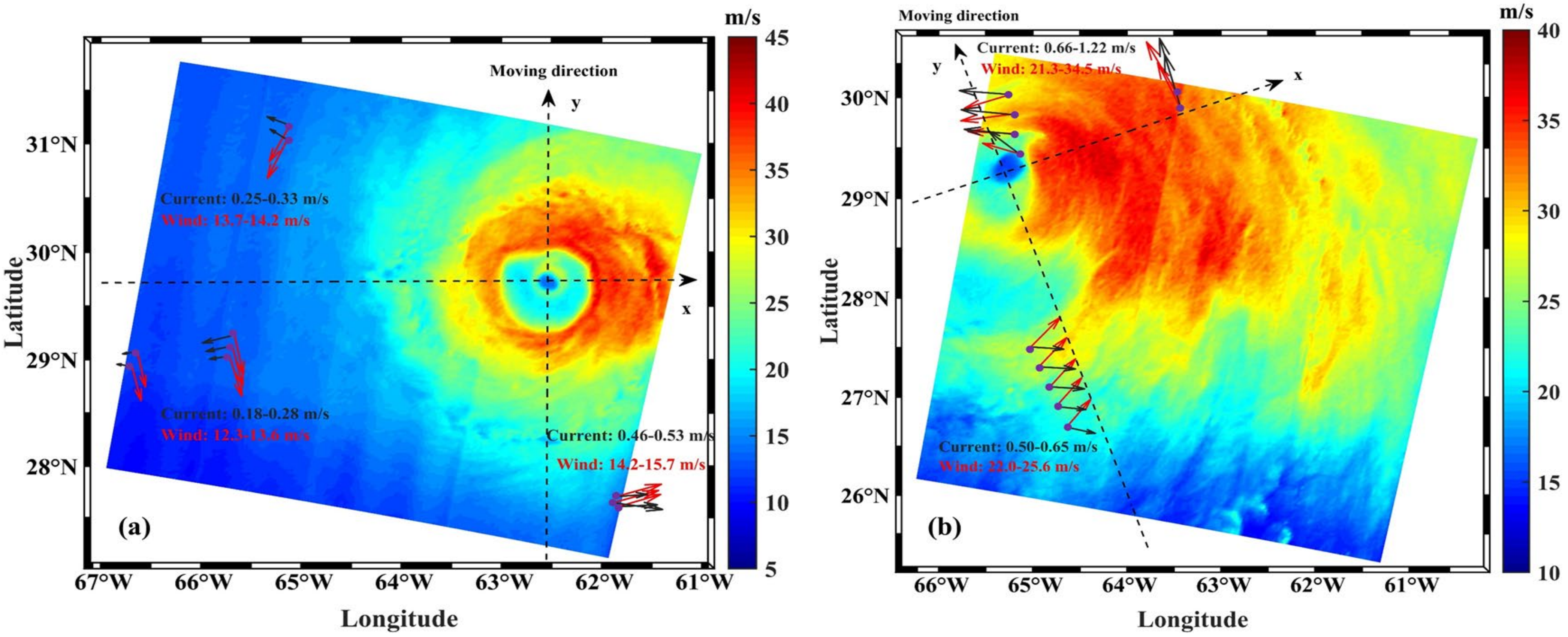

Fan & Zhang et al. 2022 JGR: Oceans

星载SAR及星座热带气旋遥感：过去，现在和将来

- In the eyewall region of Hurricane Igor, high winds (e.g., about 47 m/s) induce strong currents (about 2 m/s).

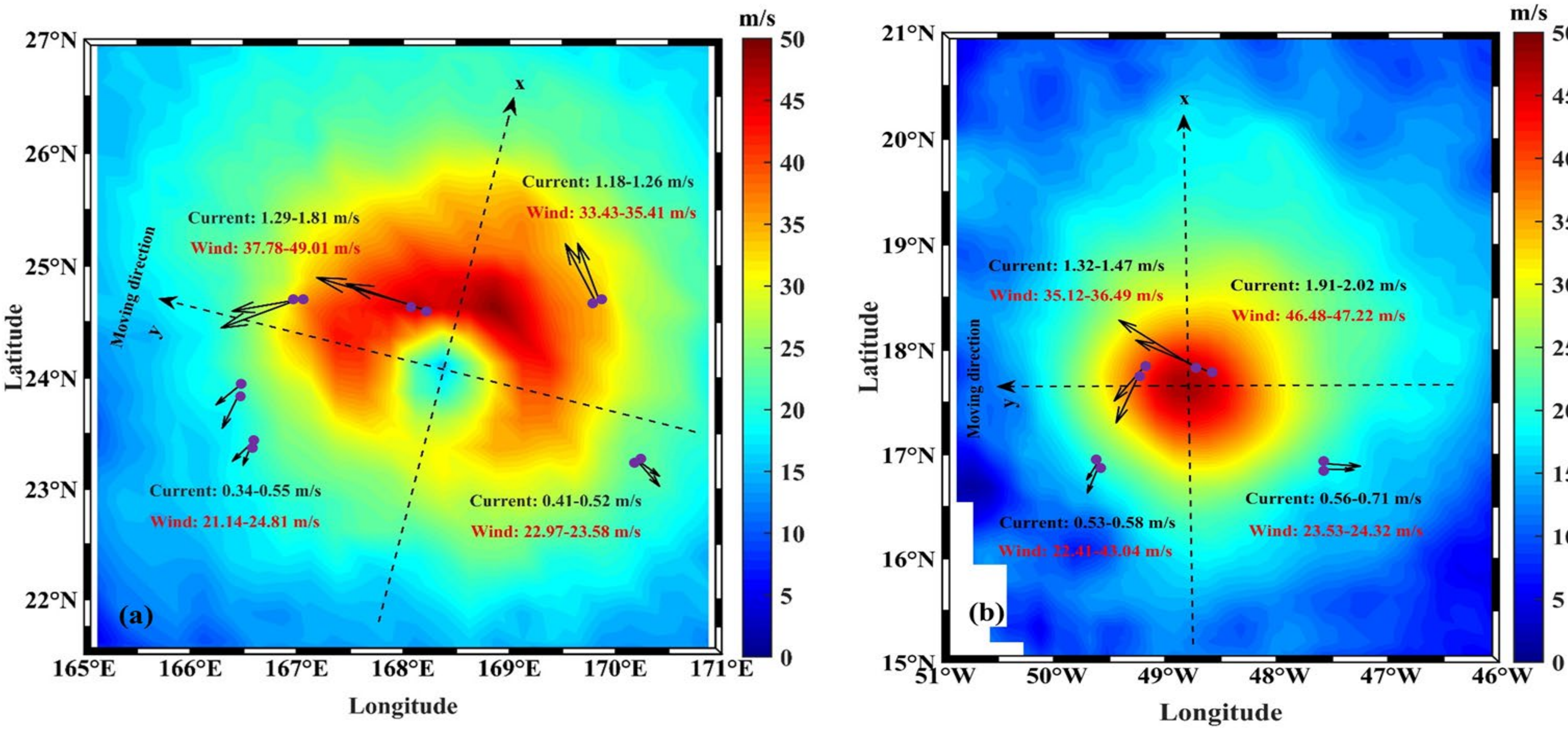

Fan & Zhang et al. 2022 JGR: Oceans

Expert insight into current research

News & views

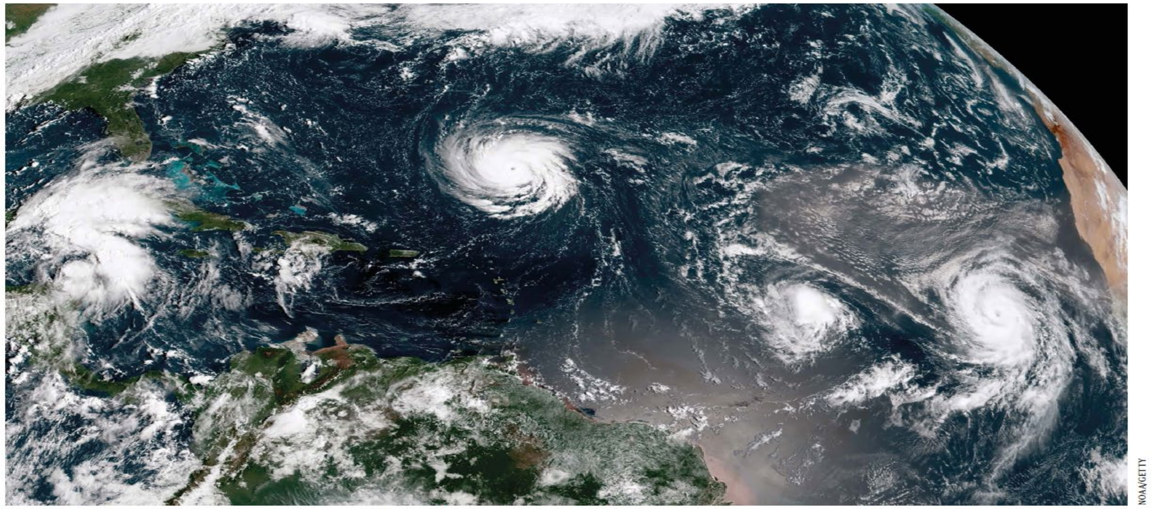

Figure 1 | Tropical cyclones over the Atlantic Ocean. Wang *et al.*[3] compiled a record of 84,110 wind-speed measurements taken during tropical cyclones that occurred between 1991 and 2020.

Climate science

Seas reveal a surge in the strength of tropical storms

Robert L. Korty

A 30-year record of ocean-current velocities has been used to infer wind speeds during tropical cyclones. The data show that these storms have intensified over time, supporting claims that their strength will increase as the planet warms. **See p.496**

Tropical cyclones, such as hurricanes and typhoons, are predicted to intensify with the temperature increases expected under current projections for global warming[1]. However, it is unclear whether historical records already show signs of this trend, because these storms form over areas of ocean that are often far from land, where direct measurements of surface wind speeds can be both dangerous and impractical to obtain[2]. On page 496, Wang *et al.*[3] report that the intensity of surface winds can be inferred from measurements of the ocean currents that build beneath them. The authors' data show that, over the past 30 years, tropical storms have grown stronger in all ocean basins in which they occur.

Warm ocean waters provide the conditions necessary for tropical cyclones to form, delivering energy that drives these storms as heat and moisture are transferred to the atmosphere. Aircraft can be used to drop instruments that measure the surface winds of a storm while it is at sea, and although the data collected provide invaluable information about the strength of tropical storms, such methods can be used in only some cases. Drones and unmanned vessels will enable more measurements to be collected in the future, but the historical record is constrained by the limited data available. For the past 35 years, aircraft missions have been restricted mainly to storms in the Atlantic Ocean.

In the absence of direct measurements, meteorologists instead rely on estimates derived from the analysis of satellite images[4]. This technique fills the void remarkably well[5], but it is nevertheless subject to biases and uncertainties, in part because it relies on subjective interpretations of the data[6,7]. These

Korty, 2022 Nature

Article

Ocean currents show global intensification of weak tropical cyclones

https://doi.org/10.1038/s41586-022-05326-4

Received: 18 February 2022

Accepted: 6 September 2022

Published online: 16 November 2022

Check for updates

Guihua Wang[1,4]✉, Lingwei Wu[1,4], Wei Mei[2] & Shang-Ping Xie[3]

Theory[1] and numerical modelling[2] suggest that tropical cyclones (TCs) will strengthen with rising ocean temperatures. Even though models have reached broad agreement on projected TC intensification[3–5], observed trends in TC intensity remain inconclusive and under active debate[6–10] in all ocean basins except the North Atlantic, where aircraft reconnaissance data greatly reduce uncertainties[11]. The conventional satellite-based estimates are not accurate enough to ascertain the trend in TC intensity[6,11], suffering from contamination by heavy rain, clouds, breaking waves and spray[12]. Here we show that weak TCs (that is, tropical storms to category-1 TCs based on the Saffir–Simpson scale) have intensified in all ocean basins during the period 1991–2020, based on huge amounts of highly accurate ocean current data derived from surface drifters. These drifters have submerged 'holy sock' drogues at 15 m depth to reduce biases induced by processes at the air–sea interface and thereby accurately measure near-surface currents, even under the most destructive TCs. The ocean current speeds show a robust upward trend of ~4.0 cm s^{-1} per decade globally, corresponding to a positive trend of 1.8 m s^{-1} per decade in the TC intensity. Our analysis further indicates that globally TCs have strengthened across the entirety of the intensity distribution. These results serve as a historical baseline that is crucial for assessing model physics, simulations and projections given the failure of state-of-the-art climate models in fully replicating these trends[13].

In addition to their tremendously destructive impacts on economy and society, TCs play an important role in the atmosphere–ocean system[14–18]. TC intensity is often defined using the 1 min, 2 min or 10 min maximum sustained surface wind speed at 10 m height. However, this parameter is not only notoriously difficult to predict, but also extremely hard to accurately estimate from observations[19]. The Dvorak technique is an empirical method widely used for estimating TC intensity from satellite imagery[20,21]. In practice, this technique first estimates a final T number (FT) from cloud patterns and infrared cloud top temperatures, then obtains a current intensity number (CI) from FT based on several rules and finally converts CI to maximum sustained wind (MSW) using a standard table. Because of the subjectiveness of the FT estimates, CI assignment and differences in the conversion table in use, the intensity estimates by different agencies can vary a lot even based on identical information[22] (Extended Data Table 1), especially for 1 min maximum wind speeds below 90 kt and above 125 kt (ref. [23]). Consequently, TC intensities in the 'best track' dataset obtained using this subjective technique have large uncertainties for trend analysis. The study in ref. [24] concluded that the total destructiveness of TCs have increased markedly over a period of 30 years starting in the mid-1970s. Based on peak intensity during a TC lifetime, the research of ref. [25] suggested that the upward trend in intensity only occurs to strong TCs (that is, categories 3–5) but not to weak TCs. It has also been found[26] that the strongest TCs (that is, categories 4–5) had increased from 1970 to 2004 in all basins except the North Atlantic. Using a new satellite-based dataset, it has been found[27] that the proportion of strong TCs increased during the period 1975–2010, whereas it has been suggested[28] that the global mean trend in TC intensity over the period 1982–2009 is statistically insignificant. Observed estimates of trends in TC intensity have not converged and the uncertainty remains large[3,11,29]. Here we develop a new approach to evaluate the changes in TC intensity during the last three decades by using huge amounts of surface drifter-derived ocean current data with high accuracy.

A close relationship between TCs and ocean currents has been identified from ocean dynamics[30], verified by various observations including acoustic Doppler current profilers[31], air-borne expendable current profilers[32], moored and drifting buoys[33], electromagnetic autonomous profiling explorer floats[34] and surface drifters[35]. Although anemometers fail to function when the air–sea boundary is not well defined, surface drifters are equipped with a drogue for nominal 15 m currents and are not strongly biased by processes at the air–sea interface (for example, winds and breaking waves). Robust evidence has been provided[36] for the near-surface current response to TCs from tropical storms to category-5 TCs. This suggests that ocean current observations can provide alternative estimates of TC intensity, given the large amounts of direct near-surface current measurements by surface drifters. Over 25,000 drifters have been deployed globally since the start of the National Oceanic and Atmospheric Administration Global Drifter Program in 1979,

[1]Department of Atmospheric and Oceanic Sciences and CMA-FDU Joint Laboratory of Marine Meteorology, Fudan University, Shanghai, China. [2]Department of Earth, Marine and Environmental Sciences, University of North Carolina at Chapel Hill, Chapel Hill, NC, USA. [3]Scripps Institution of Oceanography, University of California San Diego, La Jolla, CA, USA. [4]These authors contributed equally: Guihua Wang, Lingwei Wu. ✉e-mail: wanggh@fudan.edu.cn

Wang et al. 2022 Nature

- SAR-retrieved wind fields, along with characteristic parameters from WW3 can be used to estimate Doppler shifts caused by wind-waves and swell, based on our recently developed Doppler velocity model (Fan & Zhang et al., 2023 TGRS).

VV-pol SAR image

Doppler shift

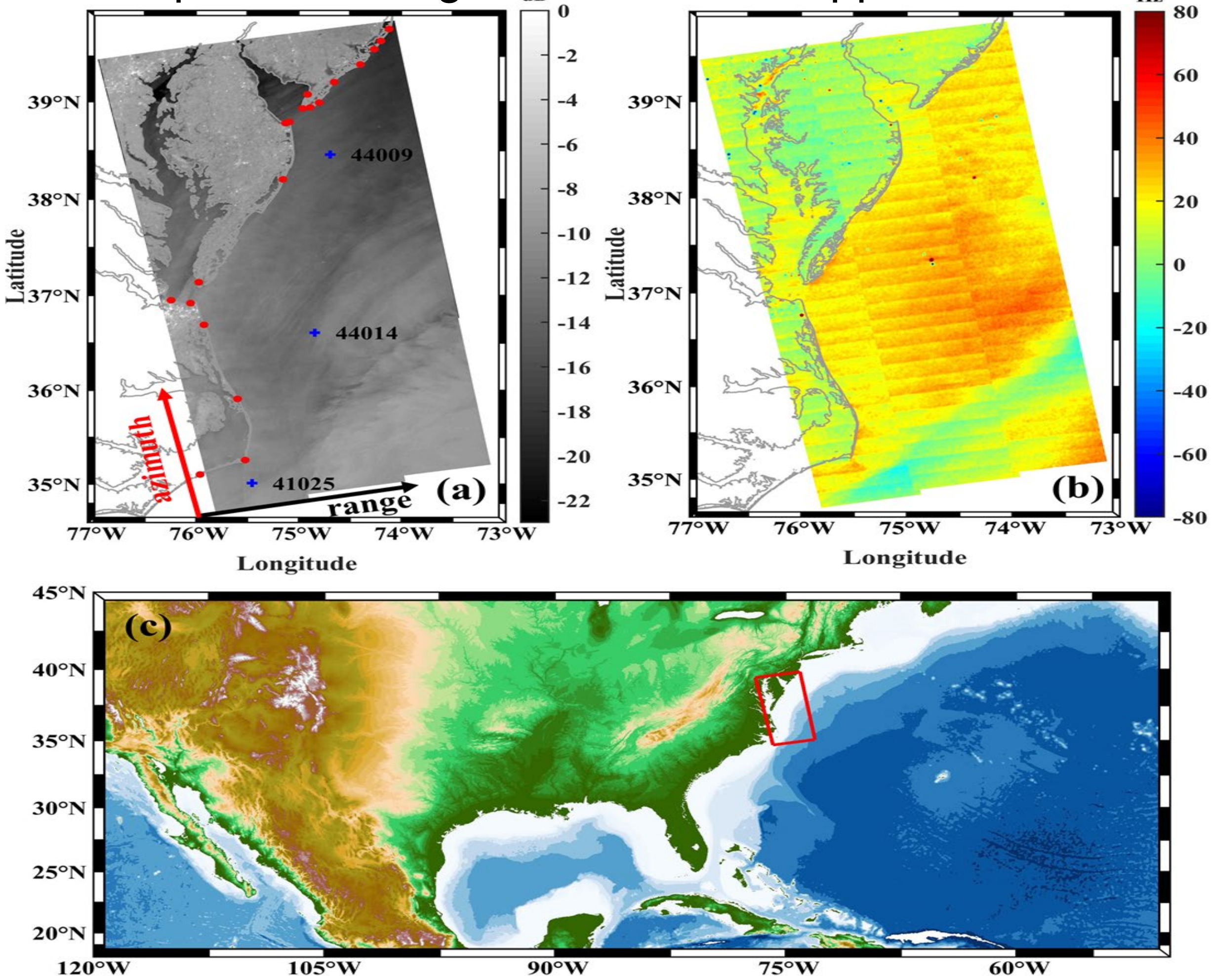

SAR winds

SWH (WW3)

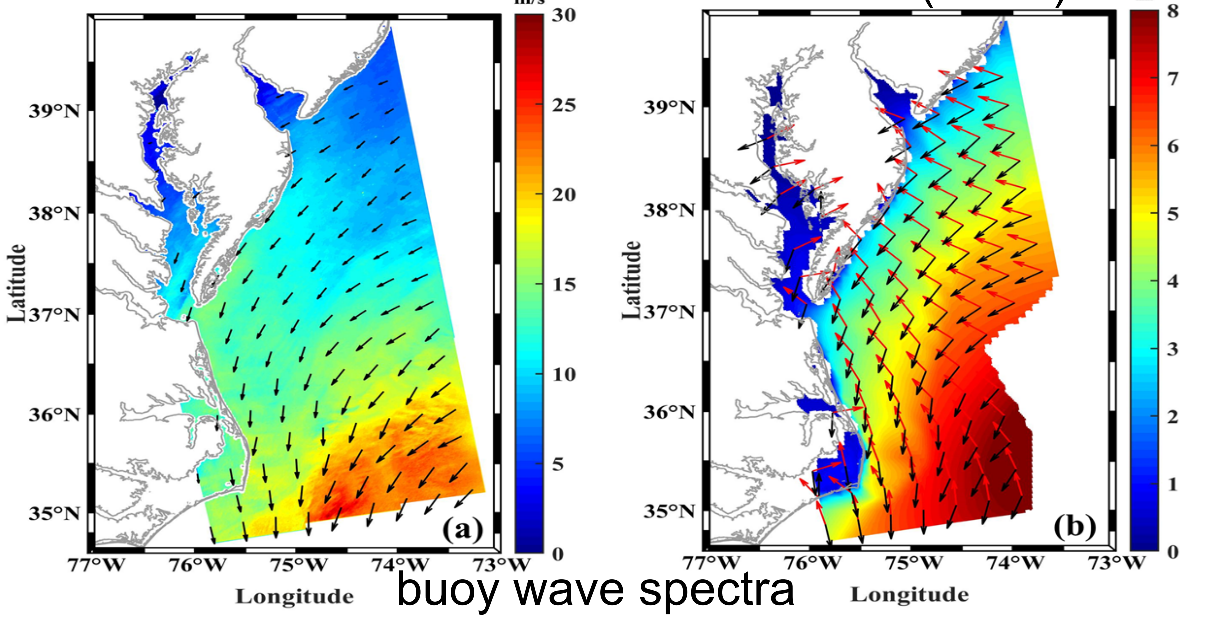

buoy wave spectra

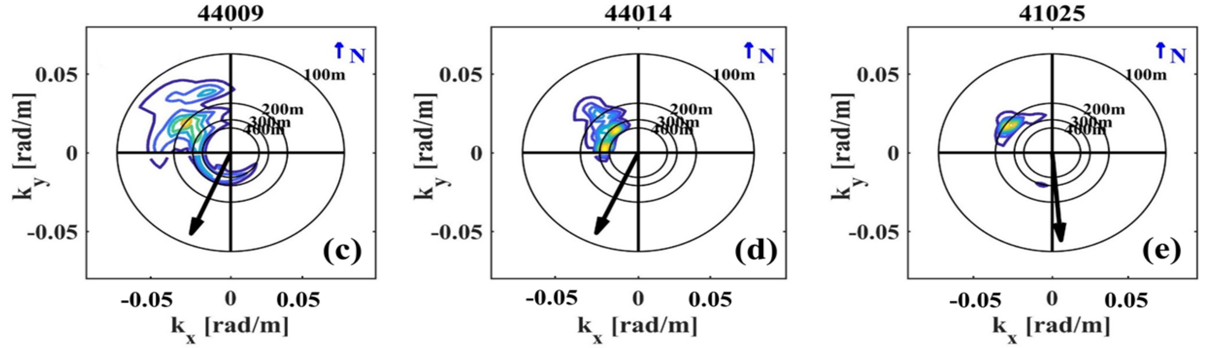

- Sea-state-induced Doppler shifts need to be accurately estimated and removed in order to obtain reliable radial ocean surface current velocities from SAR measurements.

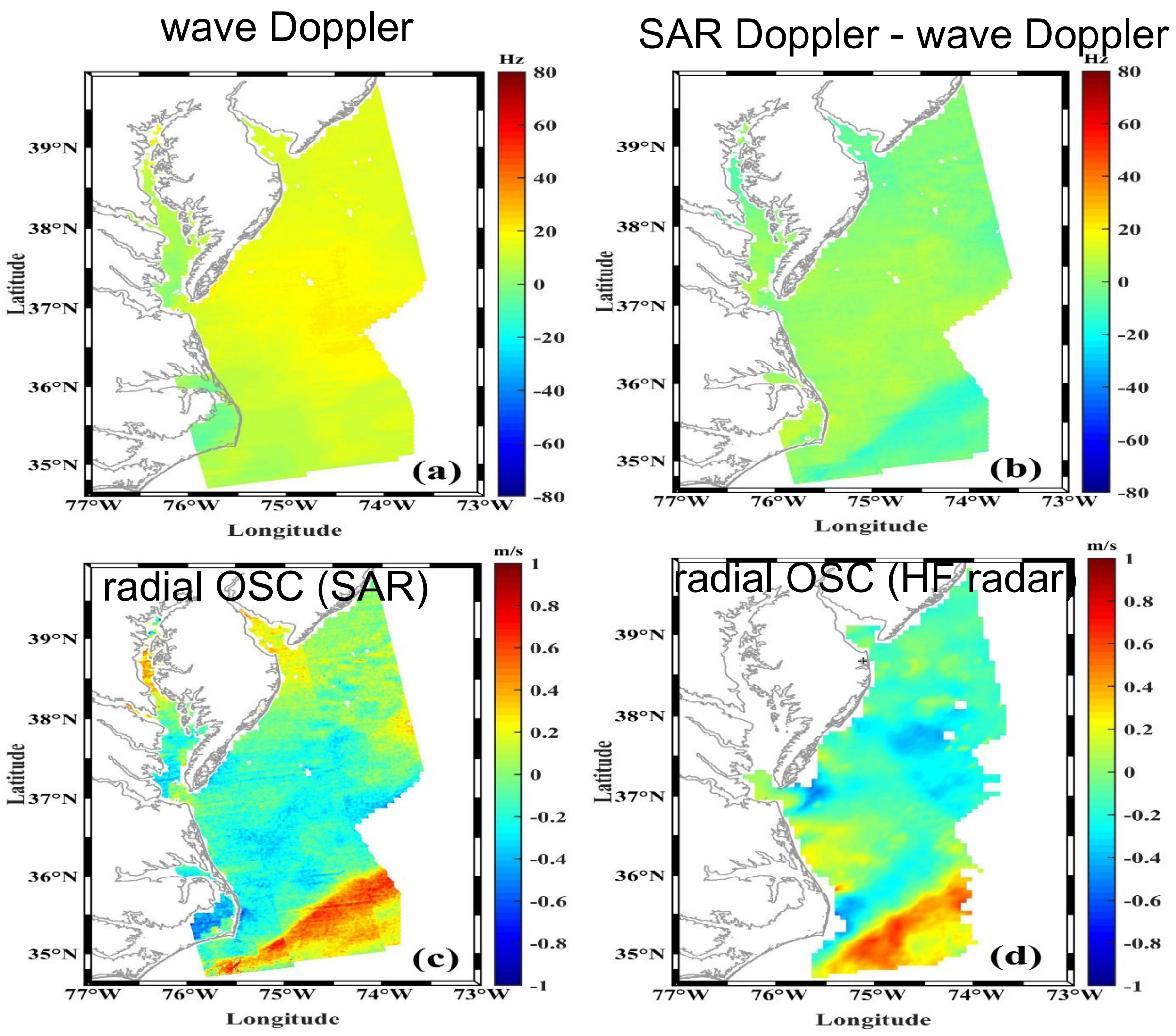

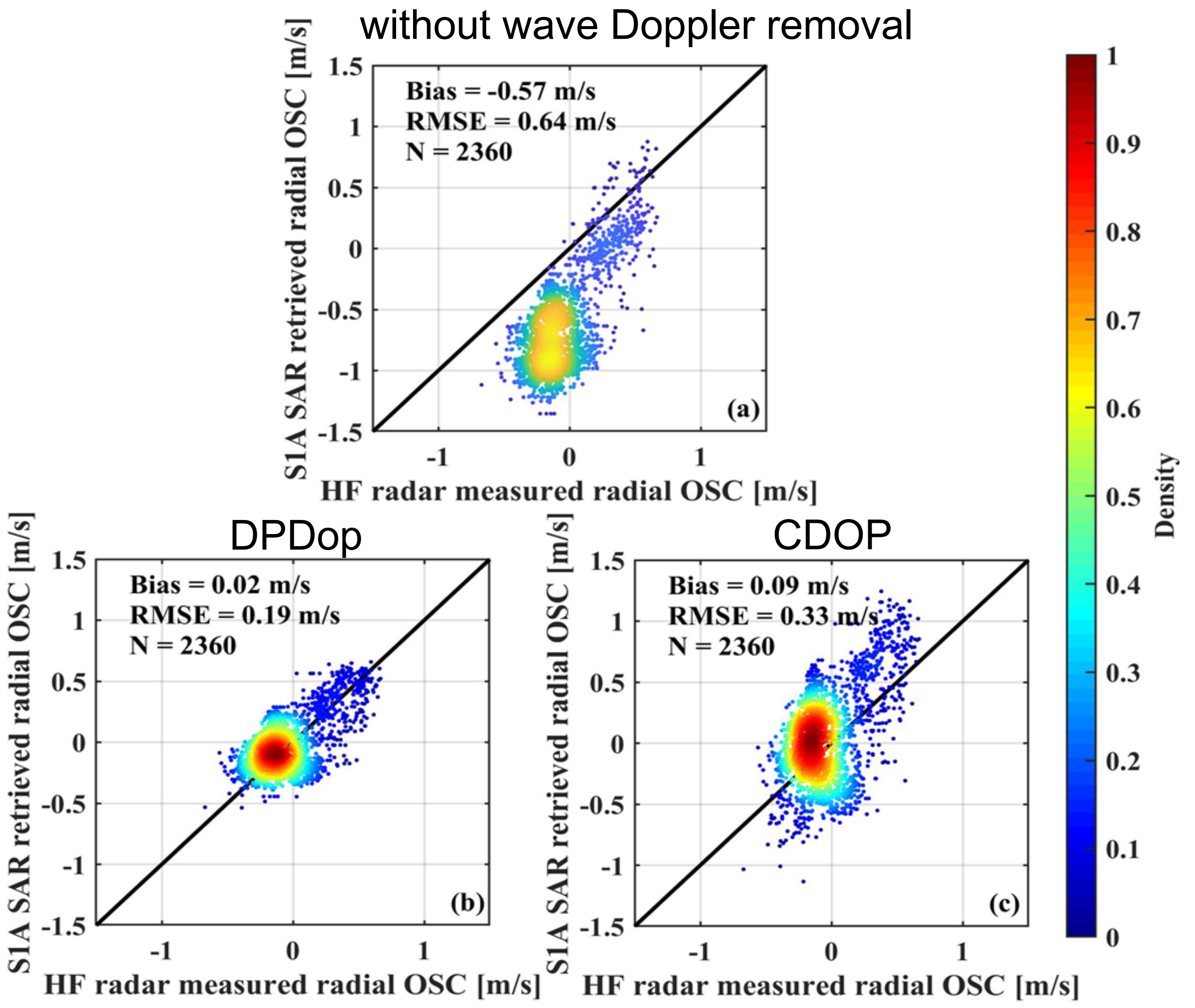

Fan & Zhang et al. 2023 IEEE JSTARS

The conventional satellite altimeters only provide one-dimensional (1D) along-track SSH observations, and the cross-track gap between two altimeter passes is large (200~300 km), especially in the tropics.

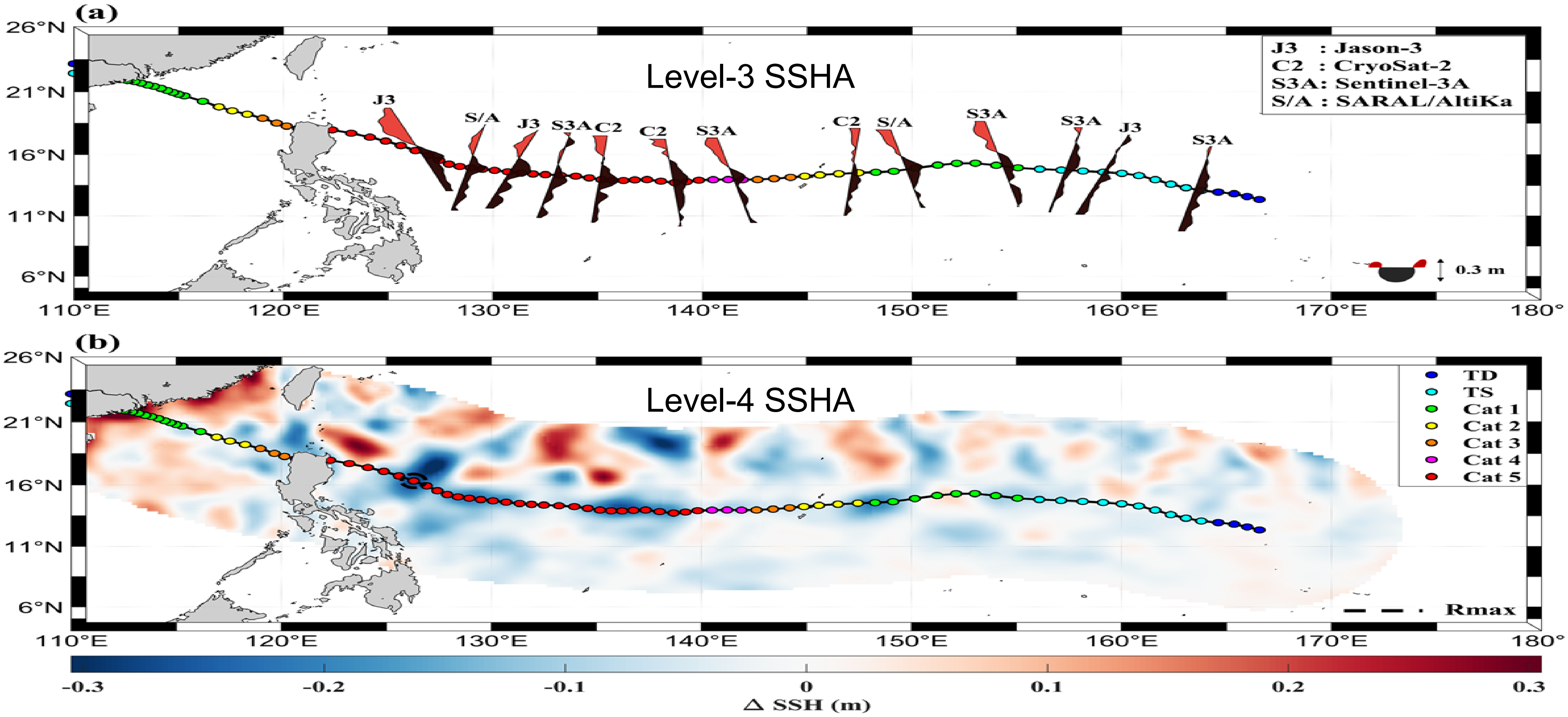

- SSH anomalies are found to be dependent on storm intensity and translation velocity.
- Larger sea surface troughs correspond to the stronger and slower moving TCs.

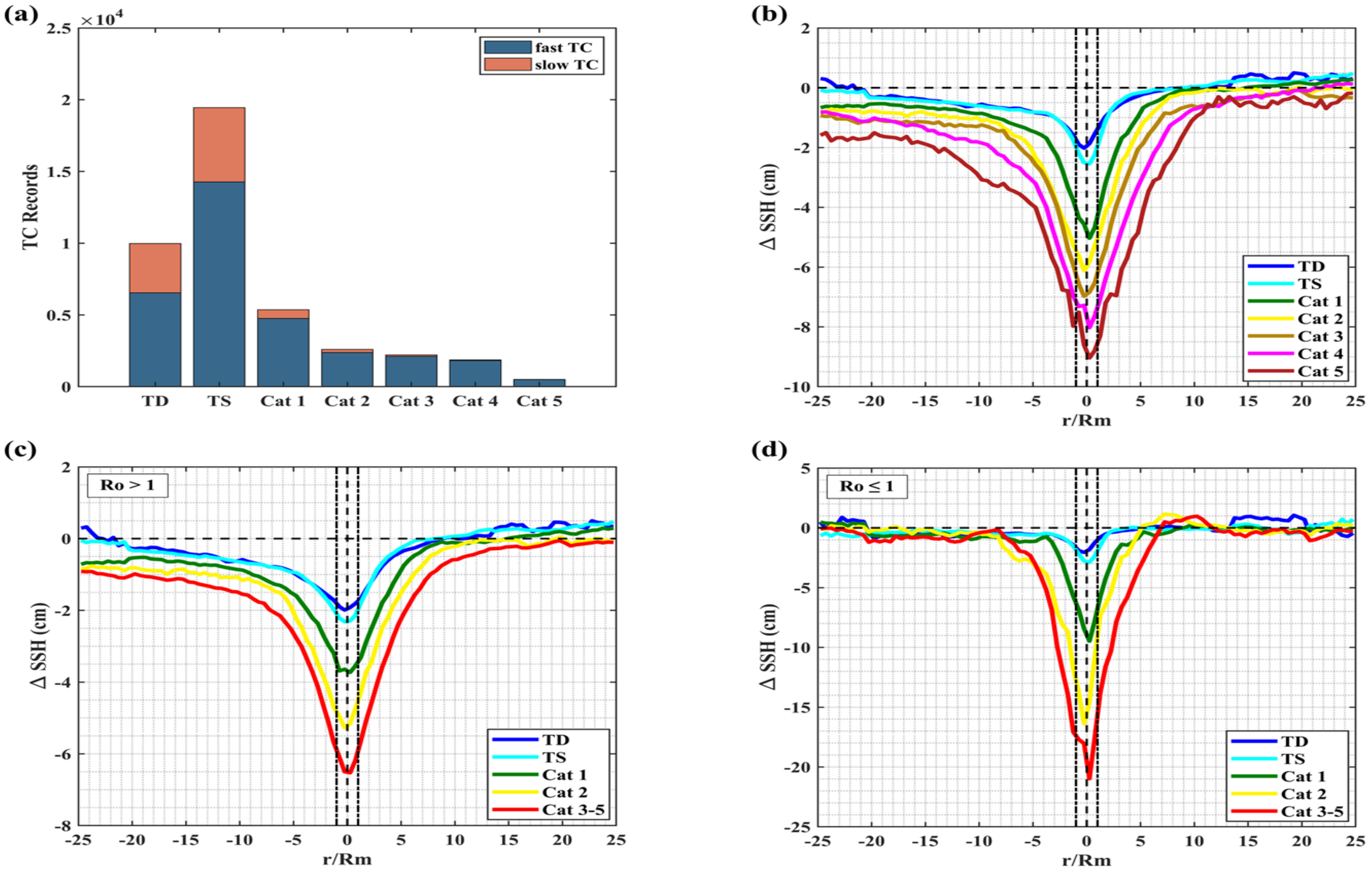

Can we estimate SSH anomalies using SAR-derived wind field parameters ?

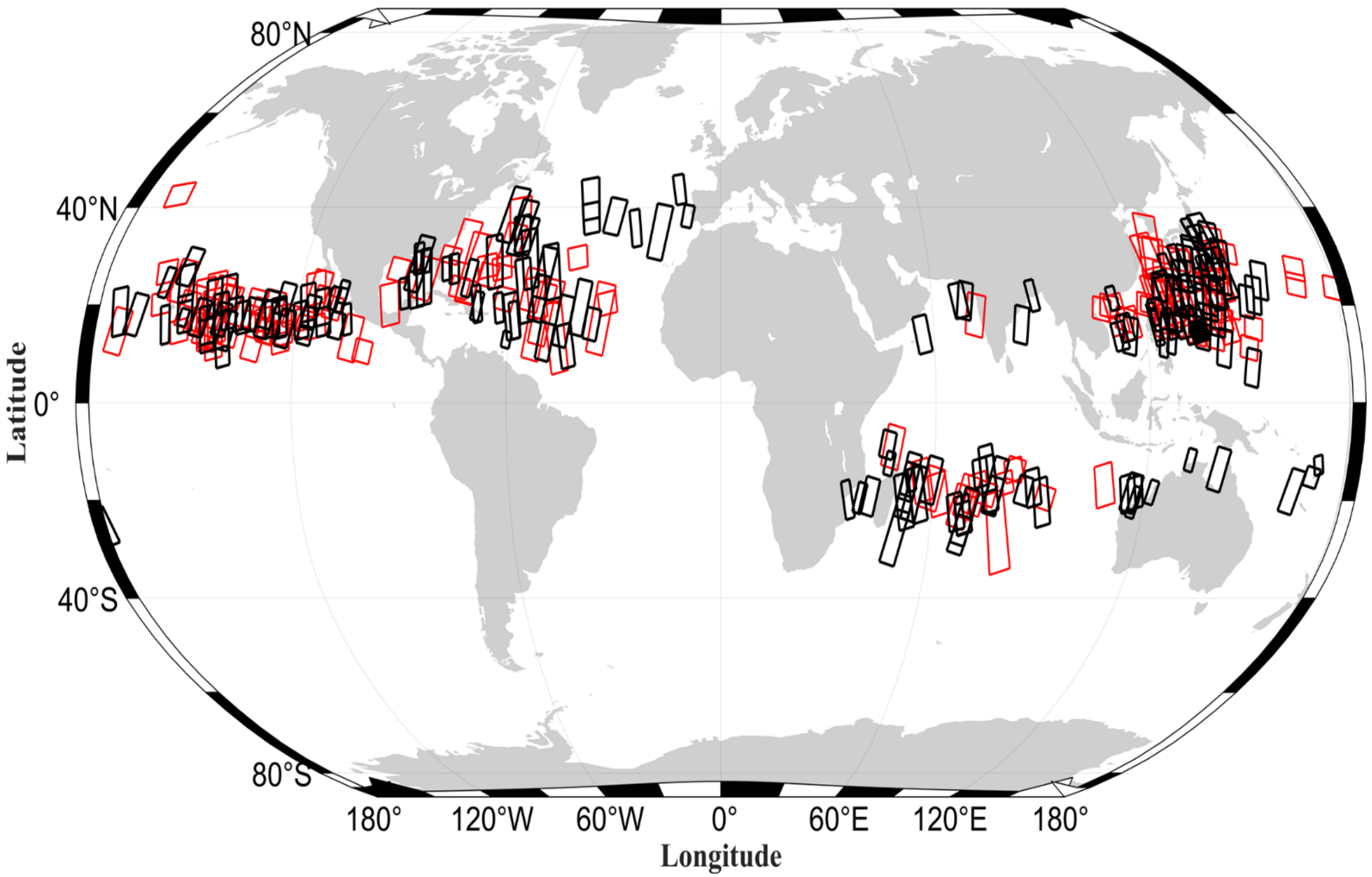

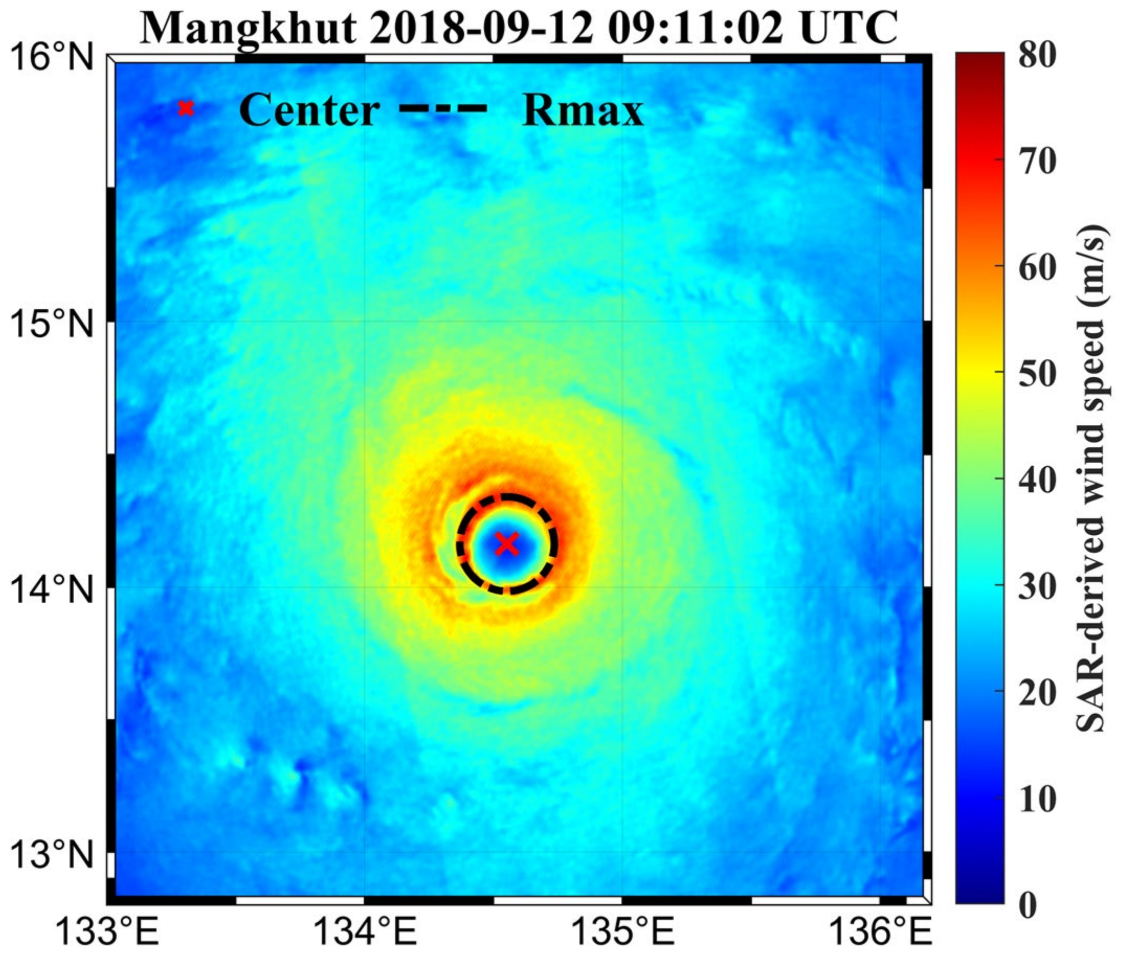

- The indirect calculations of SSH anomalies may serve as an important complement for TC inner-core areas, when altimeter observations are not available.

$$\frac{g \times SSHA}{V_m^2} \propto \frac{R_m \times N}{V_t}$$

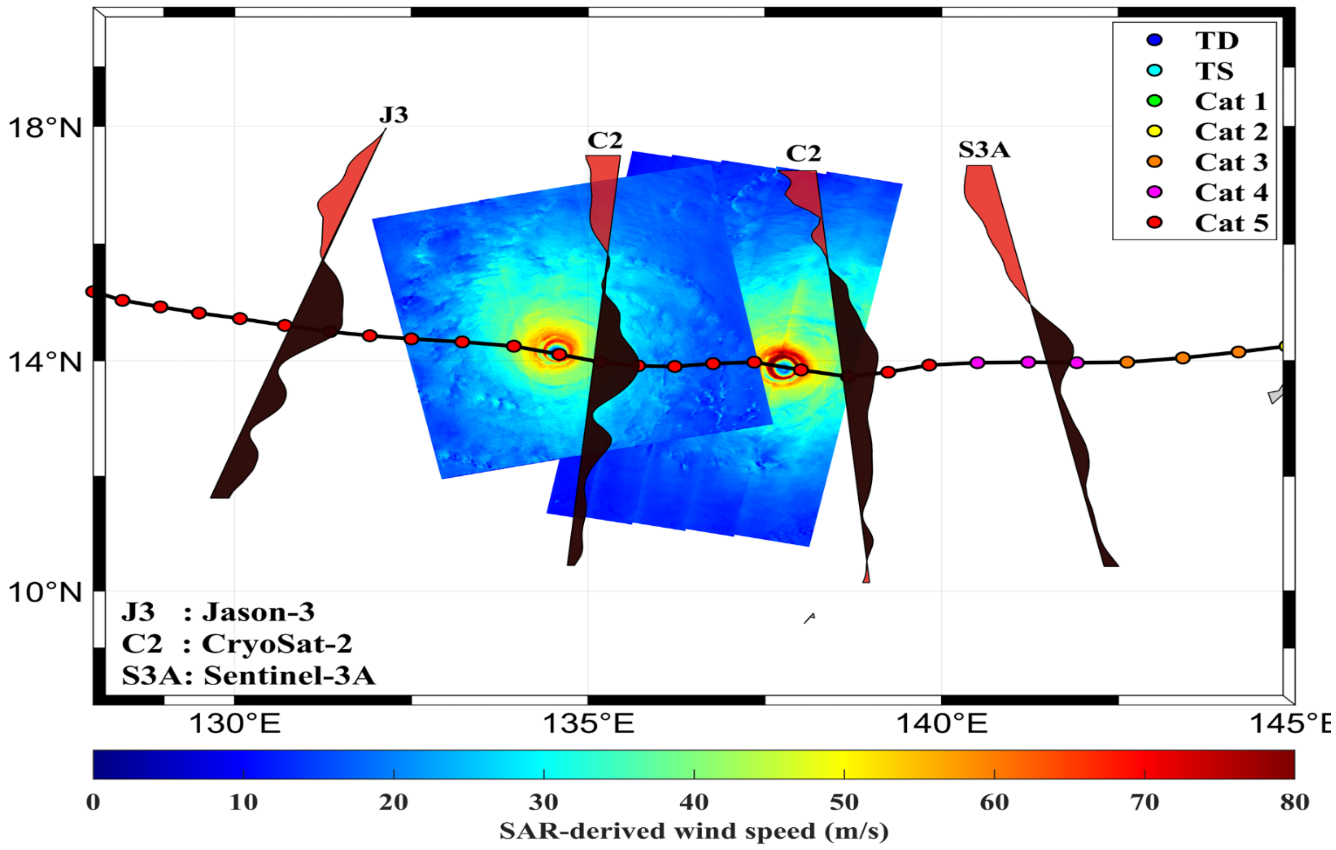

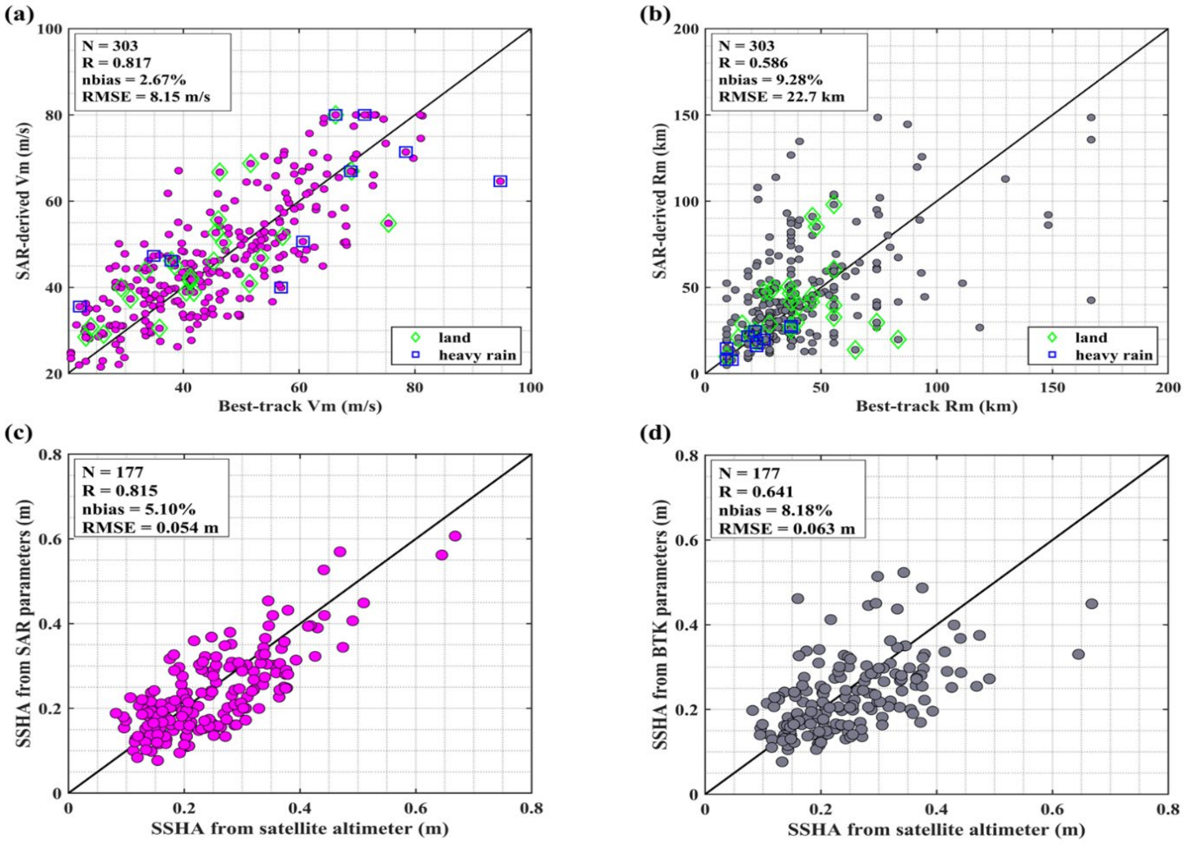

Zhang et al. 2023 IEEE TGRS

➢ Next-generation SAR constellation: “CHORUS” (multi-frequency & multi-polarization SAR)

- 700 km accessible swath width and the ability to look in left- and right-looking modes.
- With both C-band and X-band sensors oper-ating in a mid-inclination orbit.
- Near Real Time (NRT) downlink and processing from CHORUS-C, and fast tasking to CHORUS-X.

Improved access, better revisit, broader coverage, lower noise, faster data rates, and finer resolution !

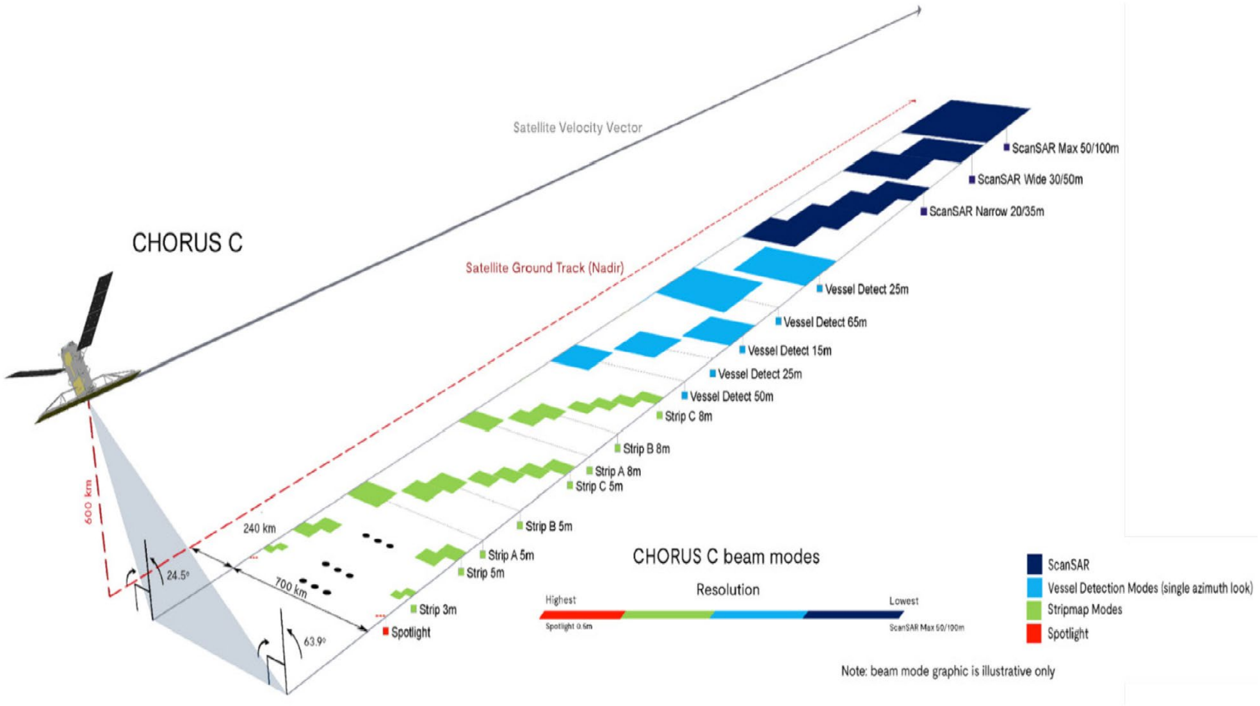

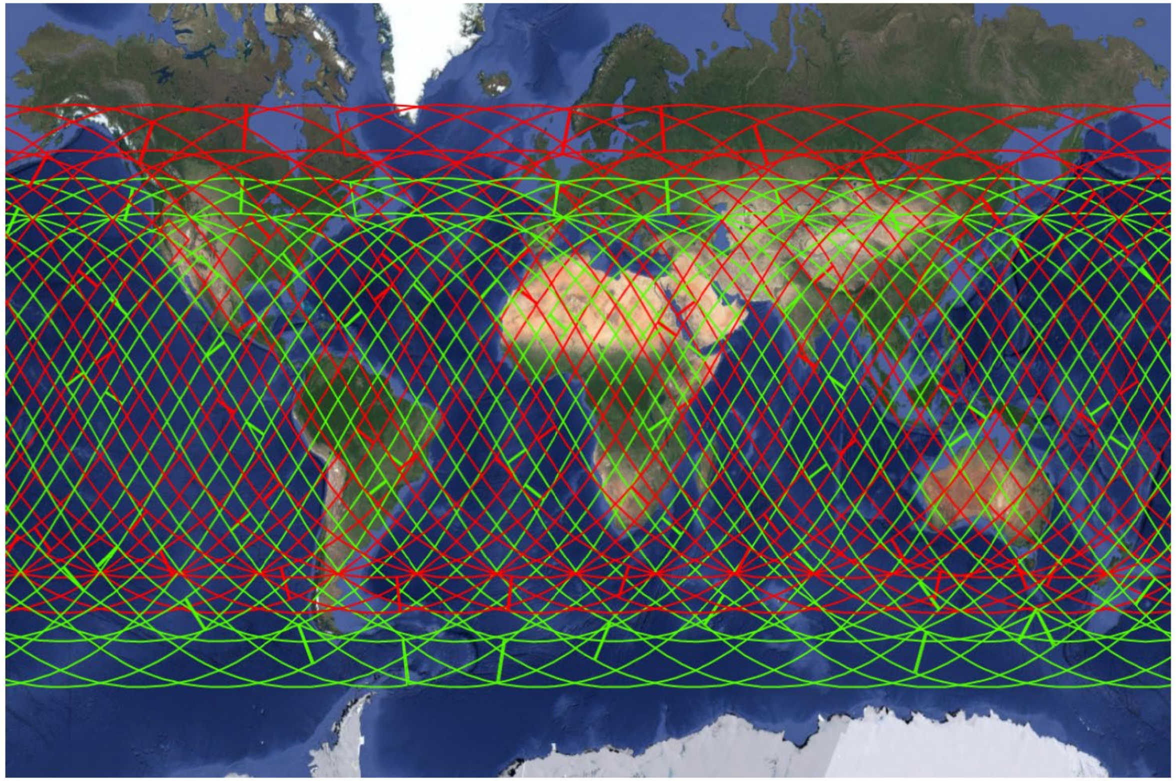

- 4R concept: real-time acquisition, real-time processing, real-time analysis, and real-time service.
- Integrated Tropical Cylone and Ocean Observation Network (ITCOON).